ELSEVIER

Contents lists available at ScienceDirect

Computers, Environment and Urban Systems

journal homepage: www.elsevier.com/locate/ceus



An integrated physical-social analysis of disrupted access to critical facilities and community service-loss tolerance in urban flooding



Shangjia Dong*, Amir Esmalian, Hamed Farahmand, Ali Mostafavi

Zachry Department of Civil and Environmental Engineering, Texas A&M University, College Station, TX 77840, United States of America

ARTICLE INFO

Keywords:

Disrupted access to critical facility Percolation modeling of urban flooding Access to service disruption tolerance index Integrated physical-social vulnerability assessment

ABSTRACT

This paper presents an integrated framework that combines a community's physical vulnerability to access disruption to critical facilities and their tolerance for such access disruption to services in order to inform the targeted communities protection and build an equitable resilience enhancement plan. The first component of the proposed framework includes a percolation simulation model capable of integrating the road network disruption probability into the flood propagation and encapsulates the road network's access to critical facilities (i.e., healthcare facilities). The discovered spatial reach of an areas' physical vulnerability dependence is 9 miles. Besides, physical disruptions in road networks and loss of access to emergency services (such as healthcare) have varying impacts on different sub-populations. To consider this aspect, the second component of the proposed framework involves a disruption tolerance index (DTI) to examine communities' tolerance towards access disruption to healthcare facilities in the face of the flooding. The proposed framework recognizes the importance of both infrastructure and human perspective of the vulnerability assessment and is tested using empirical data from Harris County, Texas, in the case of road network disruptions due to fluvial flooding. Houston, the fourthlargest city in the United States, is within Harris County. Integrated spatial analysis result reveals different spatial clusters of vulnerability across the study region and provides important insights regarding the critical infrastructure protection prioritization and hazard mitigation planning. The spatial clusters also unveil the existence of a homogeneous spatial pattern where similar vulnerable areas stay together. The proposed framework could be adopted by other cities and different critical facilities to enable decision-makers, infrastructure managers, and city planners to better evaluate their community vulnerability.

1. Introduction

Among the most catastrophic disasters, floods have been causing extensive losses during the past decades. Climate change, extreme rainfall, and sea-level rise greatly affect the frequency and severity of flood hazards. Due to the growing urbanization and economic assets development in flood-prone areas, by 2050, the global exposure to floods is expected to increase by a factor of three (Aerts et al., 2018). This growing flood risk presents significant threats to lifeline infrastructure networks whose functions support community well-being. Roadways, in particular, have an important role in transporting people and goods, evacuating people from impacted regions, and providing access to resources and services for the impacted populations. Disruptions in roadways cut off access to critical facilities such as shelters, healthcare facilities, and police and fire stations, and hence, endanger the lives and safety of populations. To better understand the increasing

risks and proactively mitigate impacts on communities, a quantitative flood-risk assessment that can systematically estimate roadway robustness, as well as vulnerability of people and assets is needed to inform hazard mitigation, investment decisions, and prioritization of improvement projects.

Roadway network robustness delineates the capability to provide access to various destinations when the network is subject to disruptions such as flood inundation. If we model a roadway network as a graph where nodes represent the intersections and links are the roads, a disruption due to flood inundation can be represented as the removal of links and nodes. Accordingly, percolation theory allows the analysis of network robustness under link and node disruption. In the percolation approach, network robustness is measured by the topological connectivity using the size of largest connected component in the aftermath of network disruption (Wang, Yang, Stanley, & Gao, 2019). Various studies (Dong, Mostafizi, Wang, Gao, & Li, 2019; Wang et al., 2019)

E-mail addresses: shangjia.dong@tamu.edu (S. Dong), amiresmalian@tamu.edu (A. Esmalian), hamedfarahmand@tamu.edu (H. Farahmand), amostafavi@civil.tamu.edu (A. Mostafavi).

^{*} Corresponding author.

have employed the percolation theory for examination of roadway robustness. However, the examination of roadway robustness based on the largest connected component neglects the fact that components in infrastructure networks can be isolated. A roadway network is robust if it maintains access to critical facilities to support the healthy functioning of society. For example, if a community's access to a healthcare facility is disrupted due to road inundation, affected people cannot receive timely medical treatment and their health and safety will be at risk. Without inclusion of critical facilities, roadway network robustness measurement would lead to inaccurate estimation of a community's vulnerability to network disruptions. In this paper, we use a novel robust component, which is the integrated size of the clusters connected to the identified critical facilities (e.g., healthcare facilities), as the measure of network robustness under flood hazards. The proposed framework evaluates the extent to which critical facilities remain accessible under flood-induced disruptions. The underlying premise of this approach is that if a node is included in the robust component, the neighborhood can reach the critical facilities. The proposed robust component approach also captures a community's needs by considering the access to multiple critical facilities, an extension of the singular origin-destination pair discussed in existing studies (Chen, Yang, Kongsomsaksakul, & Lee, 2007; Chen, Yang, Lo, & Tang, 2002; Poorzahedy & Bushehri, 2005; Sakakibara, Kajitani, & Okada, 2004). In addition, the proposed framework considers that disruptions in infrastructure networks are not random (which is an assumption made by many network robustness studies). For example, roads located in the floodplain and closer to the flood channels are exposed to higher risks and have higher disruption probability. Moreover, we employ a probabilistic percolation approach that incorporates the spatial flooding risks into simulating the likelihood of network disruption. The spatial probabilistic nature of infrastructure failures is thus captured in the proposed framework.

While evaluation of road network robustness informs about the physical vulnerability of communities, the outcomes do not inform about the societal impacts of flood induced disruptions. Network assessment based purely on physical robustness/vulnerability assumes a uniform behavior within the communities, which neglects the fact that different sub-populations of community use and rely on the infrastructure and respond to disaster impacts in different ways. In fact, socially vulnerable populations (the poor, racial minorities, and people with disabilities) are shown to experience disproportionate risk due to disaster impacts such as infrastructure disruptions (e.g., power outages, and road closures) (Charles, 2003; Peacock, Dash, & Zhang, 2007; Zahran, Brody, Peacock, Vedlitz, & Grover, 2008). For example, black households have constrained access to hurricane preparedness supplies (Peacock, 2003); socially vulnerable populations have proven to experience more casualties during flood events in Texas (Zahran et al., 2008). Recognizing this, we conclude that the current body of knowledge lacks the integration of physical-social aspects in the community vulnerability assessment. This knowledge gap has inhibited translation of network disaster resilience research to community actions aimed at reducing risk disparities in hazard mitigation planning and prioritizing infrastructure protection. Recent studies (Aerts et al., 2018; Cutter, Emrich, Morath, & Dunning, 2013) have attempted to integrate general measures of social vulnerability (such as the social vulnerability index) along with physical infrastructure vulnerability. Measures of social vulnerability, however, do not fully capture the extent to which a certain sub-population group could tolerate disruptions to particular infrastructure services. In other words, impacts of infrastructure service disruptions on different vulnerable sub-populations are not homogeneous (Esmalian, Dong, Coleman, & Mostafavi, 2019, Esmalian, Ramaswamy, Rasoulkhani, & Mostafavi, 2019; Coleman, Esmalian, & Mostafavi, 2019; Dargin & Mostafavi, 2019). To address this limitation, this paper proposes a new measure, disruption tolerance index (DTI), to capture the extent to which disruption in a particular infrastructure influences certain sub-populations. In particular, a healthcare service DTI is determined to characterize a community's vulnerability to losing access to healthcare facilities in the face of flooding. To construct the DTI, various influential factors are identified using a post-Harvey household survey. These factors are aggregated at the census tract level to determine a location-specific DTI. The calculated location-specific DTI values are utilized in conjunction with the simulated road network robustness results to classify urban areas into different categories of physical and social vulnerability. This information provides important insights for prioritization of infrastructure projects and hazard mitigation actions.

This research is primarily motivated by the fact that either physical or social vulnerability alone does not offer sufficient information to characterize communities' risk of disrupted access to critical facilities in flooding. The proposed framework contributes to the state-of-the-art research on infrastructure resilience and flood risk reduction by proposing an integrated analysis approach considering both physical vulnerabilities due to flood-induced disruptions and people's tolerance of service disruptions. The employed robust component analysis overcomes the limitation of previous network percolation models where only road network topology is considered. In addition, the analysis of physical vulnerability in this framework involves considering the inundation probability of roads based on spatial flood hazards to provide a more realistic flood disruption scenario. Also, the proposed framework identifies the important socio-demographic factors that influence people's tolerance to healthcare facilities inaccessibility. These factors are used to determine the disruption tolerance index at the census tract level. The proposed integrated framework also provides invaluable policy implications for hazard risk reduction. First, the proposed framework is able to identify the critical areas that are physically prone to access disruption to healthcare facilities due to road inundation. These areas should be highlighted for transportation planning so that the critical roads are prioritized for hazard mitigation and protection, such as retrofitting and road elevation. Second, the identification of communities that are socially intolerant to access loss to healthcare facilities suggests the inclusion of peoples needs in the critical facility sitting decision-making, such as relocation of existing healthcare facilities or the development of new healthcare facilities. Third, the detection of the hot-spots of vulnerable communities can inform the emergency response planning by prioritizing those areas for resource allocations in order to reduce the societal impact of access loss to services in urban

The remainder of the paper is organized as follows. Section 2 presents a review of the existing research related to roadway network robustness modeling and social vulnerability assessment. Section 3 introduces the elements of the proposed integrated physical-social analysis framework. The application of the proposed analysis framework is shown in a study of Harris County. Section 4 presents the percolation analysis on the flood disrupted access to critical facilities, and the spatial reach of the physical vulnerability dependence of regions is discovered. Section 5 presents an examination of household tolerance to disrupted access to healthcare services using a survey of Harris County residents in the aftermath of Hurricane Harvey, and the spatial clusters of the vulnerable areas are detected. Subsequently, the identification of important social factors and determination of disruption tolerance index (for healthcare services) for different areas are discussed. Section 6 presents the integrated physical-social vulnerability assessment through spatial analysis. Finally, section 8 discusses the significance of the proposed framework and findings.

2. Literature review

2.1. Roadway network robustness modeling

Network robustness analysis is often associated with the investigation of physical vulnerability, reliability, and accessibility (Jenelius & Mattsson, 2015; Sullivan, Aultman-Hall, & Novak, 2009). Vulnerability describes the degree of network performance decrease due to perturbations (Holme, Kim, Yoon, & Han, 2002; Jenelius, 2009; Sullivan et al., 2009). Roadway network vulnerability, in particular, refers to the "susceptibility to incidents that can result in considerable reductions in roadway network serviceability" (Berdica, 2002). In other words, the concept of vulnerability can be considered as the reciprocal of robustness (De Oliveira, Da Silva Portugal, & Junior, 2014; Iyer, Killingback, Sundaram, & Wang, 2013). In this study, since we mainly focus on investigating disrupted access to critical facilities during flood inundation. The network performance reduction is measured by the number of nodes that lose access to identified critical facilities, such as healthcare facilities. Reliability refers to the probability that a given element in the system can maintain satisfactory functionality at any given time (Mattsson & Jenelius, 2015; Murray & Grubesic, 2007). Reliability analysis consists of three categories: connectivity reliability (the probability of a node stays connected), travel time reliability (the probability that a trip is made within a specified time interval), and capacity reliability (the probability that a network can successfully accommodate a given travel demand) (Murray & Grubesic, 2007; Sakakibara et al., 2004). There are also many studies that use measures such as response time change (Tamima & Chouinard, 2017), travel cost (Nagurney & Qiang, 2009), traffic delay (Ganin et al., 2017), vehicle miles traveled (VMT) increase (Dehghani, Flintsch, & McNeil, 2014), and operation efficiency loss (Church & Scaparra, 2007). These measures are closely tied to accessibility analysis, which studies "the relative ease of reaching various services, destinations, and/or activities from a particular origin" (Kwan & Weber, 2008; Novak & Sullivan, 2014; Vandenbulcke, Steenberghen, & Thomas, 2009). Östh, Reggiani, and Galiazzo (2015) investigated the municipality's economic functioning combining socio-economic resilience with accessibility measures. The standard analysis of accessibility based on mobility relies on empirical traffic data for modeling and calibration (Jenelius, 2009; Jenelius & Mattsson, 2015; Tahmasbi & Haghshenas, 2019); daily travel demand is often adopted. Due to the stochastic nature of natural disasters, however, post-disaster travel demand data is different from that of normal behaviors. Therefore, these mobility-based frameworks have limitations for assessment in the context of hazards study (Ganin et al., 2017). In addition, traffic engineering models tend to focus on a single pair of origin-destinations (Novak & Sullivan, 2014). However, in a disaster setting when critical services are needed and critical facilities are sought, we need to consider multiple suitable destinations (i.e., critical facilities) instead of individual ones. The robust component adopted in this paper overcomes these limitations by incorporating all critical facilities into the search fields and informing on the existence of access to any suitable facilities. Also, network disruption is a stochastic event, as opposed to the deterministic failure that often studied in traffic engineering models. Chang and Nojima (2001) pointed out that post-disaster studies require performance measures that emphasize physical conditions and network functionality. Wang et al. (2014) found that vulnerability estimation that ignores network topologicalrelated factors and only focuses on traffic-related factors would be limited in providing true insights regarding vulnerability. Thus, in this paper, we use a topology-based modeling and simulation method to investigate the county-wide road network performance under different scales of flooding. The adopted topology-based modeling examines physical vulnerability (or robustness) based on percolation theory. The graph-based network vulnerability analysis approach assumes people's movement in the post-flood scenario is bounded by the road network, which to some extent excludes possibilities of off-road navigation in a flooded landscape (Helderop & Grubesic, 2019). Besides, the vehicle may be able to navigate through a shallowly inundated road (Pregnolato, Ford, Wilkinson, & Dawson, 2017; Price & Vojinovic, 2008; Yin, Yu, Yin, Liu, & He, 2016). While the off-road travel and inundation depth are not considered in the proposed framework, the network-based road vulnerability analysis is still meaningful and provides valuable insights because the post-disaster movement is mostly road-based. Hence, examining disrupted access to critical facilities based on road network vulnerability enables criticality-prioritized transportation infrastructure protection and risk-informed emergency planning and flood risk reduction.

Percolation theory allows examining the robustness of a network or a network-of-networks (Kulkarni, Stough, & Haynes, 2000; Wang et al., 2019). The largest connected component, known as the giant component, is measured to represent the network robustness under disruption (Motter & Lai, 2002; Schneider, Moreira, Andrade, Havlin, & Herrmann, 2011). In the context of roadway network study, percolation theory assumes an individual car can only travel in the giant component. Although this assumption stays valid when the connectivity of the network is the main concern, it is impaired when the functionality of the network relies on the resources and services that require access to critical facilities. In this case, we use the robust component, which encapsulates a nodes' access to critical facilities to measure that network's robustness (Dong, Wang, Mostafavi, & Gao, 2019; Dong, Wang, Mostafizi, & Song, 2020). In addition, the previous percolation research mainly focused on theoretical networks such as scale-free networks and Erdös-Rényi networks (Cohen, Havlin, & Ben-Avraham, 2003; Gao, Buldyrev, Havlin, & Stanley, 2011; Li et al., 2011; Radicchi, 2015) or distribution approximated infrastructure networks (Buldyrev, Parshani, Paul, Stanley, & Havlin, 2010; Crucitti, Latora, Marchiori, & Rapisarda, 2004; Radicchi, 2015). Infrastructure networks, however, show very different characteristics and spatial patterns compared to theoretical networks. For example, Dong, Mostafizi, Wang, et al. (2019) showed that degree correlation in road network violates the assumption of theoretical methods such as generating function method so that they are not applicable in analyzing the network robustness.

A simulation-based network robustness assessment approach is required to effectively examine post-disaster road network robustness performance. The existing simulation-based approaches primarily focus on analyzing network robustness under theoretical failure schemes such as random failures (Bashan, Berezin, Buldvrey, & Haylin, 2013; Dong, Mostafizi, Wang, et al., 2019), localized attacks (Berezin, Bashan, Danziger, Li, & Havlin, 2015; Shao, Huang, Stanley, & Havlin, 2015; Zhao, Li, Sanhedrai, Cohen, & Havlin, 2016), and targeted attacks (Berche, von Ferber, Holovatch, & Holovatch, 2009; Duan & Lu, 2013; Huang, Gao, Buldyrev, Havlin, & Stanley, 2011; Solé, Rosas-Casals, Corominas-Murtra, & Valverde, 2008). However, the link/node removal is often associated with disruption probabilities (Li, Dong, & Mostafavi, 2019a, 2019b). In roadway network robustness analysis, disruption of roads is not random but rather depends on geographic exposure to hazards. For example, roads in the vicinity of flood channels are more likely to flood during an extensive rainfall event. Therefore, probabilistic failure propagation (based on spatial characteristics of flood hazards) should be incorporated when assessing road network robustness. The proposed framework employs a percolation-based modeling and simulation analysis that examines the robust component as the robustness metric and models probabilistic link failures caused by flood propagation.

2.2. Social vulnerability to infrastructure disruption

Public has different expectations for infrastructure services in the aftermath of a disaster. Merely focusing on the physical vulnerability of infrastructure systems neglects the fact that the public does not experience the access disruptions equally (Grinberger & Felsenstein, 2016). Studies show that in case of a service disruption, such as loss of access to critical facilities, different subgroups of people can have varying tolerability to disruption (Petersen, Fallou, Reilly, & Serafinelli, 2018). Recent studies have shown that different sub-populations have distinct needs and expectations of the infrastructure services during and after the disaster strikes (ATC, 2016). Therefore, recognition of the tolerance disparity among different sub-populations is imperative for community-level vulnerability assessment (Martins, e Silva, & Cabral,

2012). To this end, we first need to identify the societal determinant of experienced hardship from loss of access to service for the infrastructure-related service of interest. Then, the identified influential factors need to be appropriately analyzed and integrated into the vulnerability assessment to reflect the spatial disparity of tolerance within the study area.

To identify societal determinant of tolerance to disrupted access to service, Murphy and Gardoni (2008) suggest that the tolerance of individuals is determined by their existing capabilities, a direct predictor of the functionality that is achievable with available resources. The investigation of tolerance among sub-populations should focus on variables that reflect their capability for coping with service disruption. In an empirical study, Esmalian, Dong, et al., 2019 has investigated the households experiences with power outages and showed that certain sub-populations have a lower capacity to tolerate power outages. Studies on the influence of individuals age and income show that different sub-populations would experience varying levels of impacts from transportation service disruption (Coleman et al., 2019; Dargin & Mostafavi, 2019). Moreover, Petersen et al. (2018) cite the interplay between socioeconomic characteristics of subpopulations and their infrastructure services needs and tolerability.

Many studies have investigated how the sociodemographic characteristics of sub-populations influence their ability to cope with disasters. It is generally agreed that socially vulnerable population are those with limited resources to cope with the threats of natural disasters (Paton, McClure, & Bürgelt, 2006). To scrutinize the concept of social vulnerability, Cutter, Boruff, and Shirley (2003) state that the main cause of the social vulnerability is inequality that reduces the capacity of certain sub-populations to respond to and recover from disasters. The inequality may be in the form of inaccessibility to resources, beliefs, customs, building stock, physical limitations, and age of individuals (Cutter et al., 2003; Perry, Lindell, & Tierney, 2001; Tierney, Lindell, & Perry, 2002). Factors that influence the tolerance to the loss of access to service include household income, lack of vehicle, disability, and age, An empirical investigation of the relationship between the perceived tolerance to loss of service and sociodemographic characteristics of individuals is needed in helping us understand the influence of different social factors for specific service disruptions.

An integrated vulnerability index quantifies the tolerance to access disruption to the service of a community as a whole. Among various methods in risk and disaster literature for considering the social vulnerability of a community, a prevalence approach for social vulnerability quantification uses composite indicators and scores to account for multiple aspects of vulnerability (Beccari, 2016). The generation of such a composite indicator integrates different social or environmental factors. For example, Social Vulnerability Index (SoVI) (Cutter et al.,

2003), as a well-known method, uses principal components analysis (PCA) to create independent factors using a number of socioeconomic indicators including age, income, race, and education at the census tract-level. Flanagan, Gregory, Hallisey, Heitgerd, and Lewis (2011) first categorized the vulnerability variables into four groups: (1) socioeconomic status, (2) racial/ethnic groups, (3) household composition, and (4) housing style. Flanagan et al. (2011) then calculated vulnerability index at the census tract level based on the percentile ranks of the vulnerability variables and counted the number of individual vulnerability variables for which the percentile rank is 90 or higher. There are several similar methods (Anderson et al., 2019: Dwyer, Zoppou, Nielsen, Day, & Roberts, 2004; Hagenlocher, Renaud, Haas, & Sebesvari, 2018; Khazai, Merz, Schulz, & Borst, 2013) developed for assessing the risk and vulnerability of the spatial areas and providing spatially related vulnerability scores of the residents. These existing approaches studying social vulnerability include multiple social dimensions that contribute to vulnerability of sub-populations facing disasters in general. However, these social dimensions are not necessarily all related to the case of infrastructure service disruptions. In this study, sociodemographic characteristics of the sub-populations that contribute to their tolerance to disrupted access to service are identified and tested through an empirical study. A tolerance index is then developed specifically for the case of healthcare service disruption. Furthermore, studies show that households with high social vulnerability tend to co-locate in the proximity of each other and form a socially vulnerable community cluster (Cutter & Finch, 2008; Frigerio & De Amicis, 2016). The same pattern is expected to be observed in the case of tolerance to infrastructure service disruptions. The existence of the high/low tolerance clusters in the region highlights the importance of identifying such vulnerable population for better emergency response during disaster events (Adger, Brooks, Bentham, Agnew, & Eriksen, 2005; Fatemi, Ardalan, Aguirre, Mansouri, & Mohammadfam, 2017). Combining the derived DTI with physical vulnerabilities, the integrated physical-social vulnerable cluster can provide valuable insight for decision-makers regarding logistics of disaster preparation and planning for emergency response.

3. Integrated physical-social vulnerability assessment framework

As discussed, the impacts of infrastructure disruptions on communities are influenced by social and physical vulnerability, both of which vary spatially. An integrated assessment of vulnerability is needed to gain a more complete understanding of the relationship between people and the built environment surrounding them (Bevacqua, Yu, & Zhang, 2018; Mayaud, Tran, Pereira, & Nuttall, 2019) to better inform decisions made by planners, government authorities, infrastructure

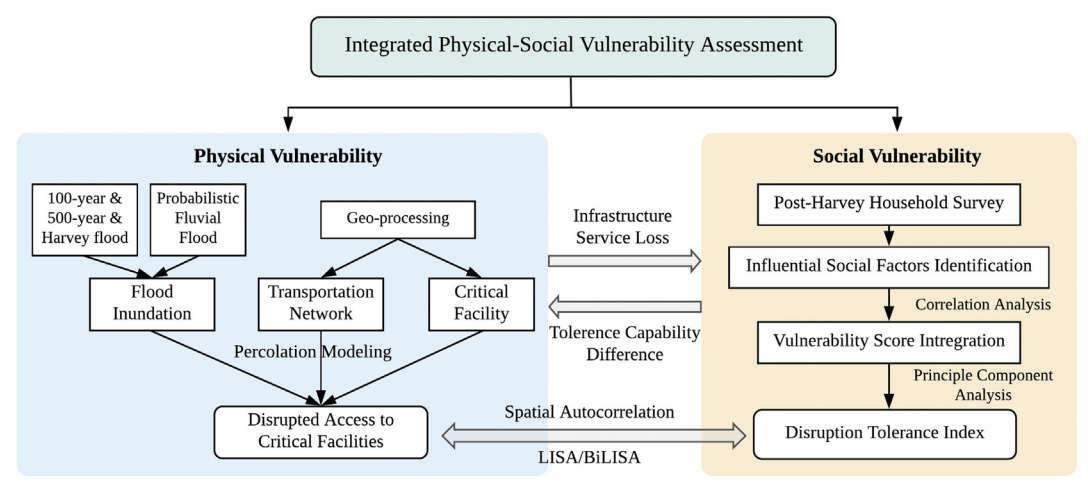


Fig. 1. Integrated physical-social vulnerability assessment framework.

managers and emergency management agencies (Ellingwood et al., 2016; Fuchs, Kuhlicke, & Meyer, 2011).

Fig. 1 illustrates two major components of the proposed vulnerability assessment framework: (1) physical vulnerability analysis that examines network's access to critical facilities during flooding, and (2) social vulnerability analysis that characterizes households' tolerance to service disruptions. In particular, the physical vulnerability analysis mainly focuses on the roadway network performance, functional status of critical facilities, and connectivity between critical facilities and communities in a flood event. Both probabilistic fluvial flooding and Hurricane Harvey flood scenarios are investigated in this study. The propagation of flood on the roadway network is modeled and simulated using a network percolation method in which the aggregated robust component size characterizes the communities' access to healthcare facilities in the face of flooding.

The second component of the framework (Fig. 1) determines social vulnerability to infrastructure disruptions. The social factors affecting residents ability to tolerate service disruptions (or disrupted access to facilities) are examined through empirical data collected from a post-Harvey household survey. Using the survey data, a principal component analysis is performed to create a disruption tolerance index for different sub-populations. Finally, an integrated physical-social vulnerability analysis is conducted to identify areas with the greatest combined social and physical vulnerability to road inundation and loss of access to healthcare facilities.

The application of the proposed framework is shown in the context of Harris County. Harris County has > 2500 miles of flood control channels and is the third-largest county in the United States. In addition, Harris County, home to Houston, the fourth-largest city in the United States, is one of the most flood-prone areas in the country. Out of 7.9 million people affected by Hurricane Harvey, 4.37 million people live in Harris County, of which 1.1 million people live in areas of high social vulnerability (America, 2017). The Hispanic population is the largest population group in the Harris County Disaster Recovery Service Area, and over 16% of the service area population has a limited English proficiency compared to 9.7% of the countys entire population. Harris County also has high concentrations of residents who are considered minorities (63.6%) or living in poverty (12.87%). Hence, Harris County provides an ideal testbed for demonstrating the application of the proposed framework and its components.

4. Analysis of flood-induced disruptions and network access to critical facilities

Our analysis examines different scenarios of flood hazards. Fluvial flooding often occurs in the area where the roads are in the vicinity of the flood control channels (rivers, bayous, and creeks). The characterization of fluvial flood hazards is usually represented by specification of floodplains. A floodplain is a geographic area along the floodways subject to flooding. The 100-year (500-year) floodplain is the land that is predicted to flood during a 100-year (500-year) storm, which has a 1% (0.2%) chance of occurring in any given year. Fig. 2 shows the roadway network map and floodplains in Harris County. Considering intersections as nodes and road segments as links, we can represent the road network of Harris County as a graph. There are in total 148,772 nodes and 203,872 links. There are 98 hospitals in total distributed across Harris County. Based on the spatial coverage, we conclude that 16.5% (33,681) of the links are within a 10-meter buffer of the 100-year floodplain, and 30.5% (62,112) of the links are within a 10-meter buffer of the 500-year floodplain. Evidently, Harris County is very vulnerable to urban flooding. In addition, the impact of flood inundation is not limited to roadway network connectivity. Flooding severely impairs people's access to critical resources and services such as hospitals, grocery stores, and pharmacies. Hence, the application of our proposed framework in the context of Harris County is geared towards understanding how robust Harris County network is in facing flooding.

4.1. Robust component: network access to critical facilities

The roadway disruptions due to flood inundation are modeled as link removal from the roadway network. The link removal is based on the failure probability ϕ that a link will be inundated, which is characterized by its distance to the waterway. To capture the network access to critical facilities under flood disruptions, we adopted the measure of robust component (Dong, Wang, Mostafavi, & Gao, 2019,Dong, Wang, Mostafizi, & Song, 2020) to examine the robustness of the roadway network of Harris County under different scenarios of flood disruptions.

The steps for determining the robust component measure are as follows (Dong, Wang, Mostafavi, and Gao (2019). In a graph G, two vertices u and v are considered connected if there is path from u to v, which is denoted as $\rho(u,v)=1$. Given a network of size N, containing K critical facilities, the connected component of k can be represented as $C_k = \{v_i | \rho(k,v_i) = 1, \forall i = 0,1,...,N\}$. The robust component of a network with failure probability ϕ can be defined as

$$\mathfrak{R}_{\phi} = \bigcup_{k=0,1,\dots,K} C_k \tag{1}$$

Fig. 3 shows the flood inundation characterized by network approach. As the overflow propagates across the network, the nodes and links will be considered nonfunctional and removed from the network (as shown in Fig. 3(b)). As the failure scale increases, the network performance will decrease and show a percolation transition. In this paper, we focus on analyzing if the nodes have access to any of the designated critical facilities. Fig. 3(b) and (c) show the change of robust component size (marked as green) when the flooding scale (marked as red) increased from $\phi = 0.02$ to $\phi = 0.3$. Road access is represented as a binary process during link removal in the percolation modeling. Once a road is (partially) inundated, we assume that the road is impassable and thus removed. In other words, even if part of a road is inundated, once the traffic enters the road, it cannot fully traverse the link. In addition, the network we investigated in this study includes fine granular data; each link is a section of a road where no other intersections can be found within a link. Hence, there is no routing diverge within a link if a road is partially inundated. The robust component is the union of the nodes with access to at least one critical facility. Regardless of the size of residual components, if they do not contain the critical facilities, they are nonfunctional and excluded from the robustness estimation (as suggested in Fig. 3(a)). More importantly, flooding disconnected communities from accessing the hospitals, despite they are not flooded themselves (as shown in Fig. 3(b) and (c) gray lines). Comparing the existing network robustness analysis that based on the centrality measures (Novak & Sullivan, 2014), a robust component enables the inclusion of all possible connections to the critical facilities rather than the shortest distance between an origin-destination (OD) pair.

4.2. Percolation modeling of near-floodway flood propagation

Extreme rainfall (such as the case of hurricane Harvey) causes fluvial flooding when rivers and channels exceed their banks (Ogie, Holderness, Dunn, & Turpin, 2018). Especially in Harris County, which encompasses multiple rivers, channels, and bayous, an examination of flood propagation on roadway networks and its impacts on the networks' access to critical facilities is of great importance. Although pluvial flooding, flood event caused by extreme rainfall is also a significant contributing factor of urban flooding, in this paper, we only focus on the fluvial flooding.

In fluvial flooding scenarios, the likelihood of road inundation is proportional to the distance to a floodway (i.e., bayou or channel). If a roadway segment is in proximity to multiple floodways, distance to the nearest floodway is considered. In total, around 7700 roads are in the range of 0 to 20 m from floodways. As the fluvial flooding often occurs in the vicinity of the floodway, this paper assumes that the closer to the

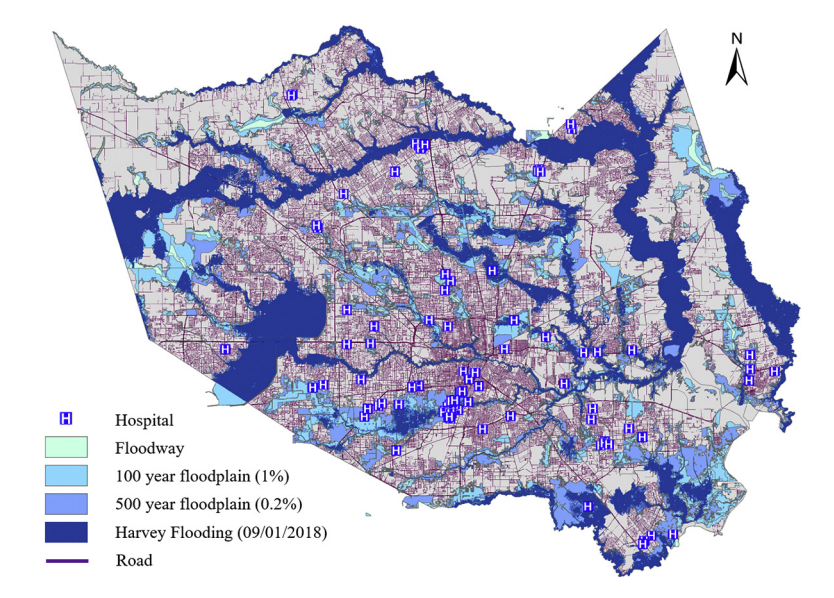


Fig. 2. Harris county floodplain map, Harris County.

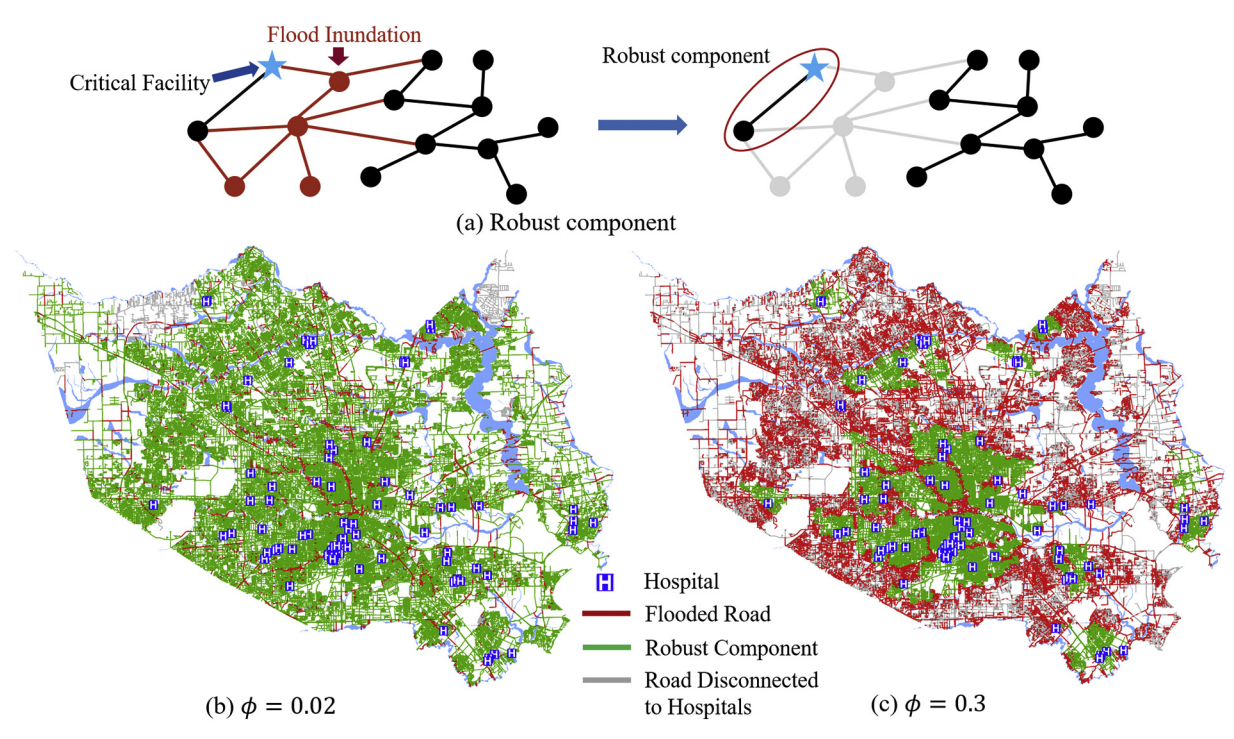


Fig. 3. Illustrative example of flood propagation on roadway.

floodway, the greater the likelihood of road inundation. The elevation of flood control and road infrastructure can also influence the scale of the flooding. However, infrastructure elevation is not incorporated in this study as the goal of the flood percolation study is to reveal the immediate impact of near-floodway roads' inundation on overall network access to critical facilities. In this case, the infrastructure elevation will have a minor impact on the results. Many other factors, such as street network topology, stormwater drainage system, and imperviousness can all influence the flood propagation. Future development can be built upon the proposed fluvial flood percolation model for extensive investigation of more scenarios. To devise the flooding scenario, we first convert the distance of roads from floodway (d_i) to flood inundation likelihoods (l_i).

$$l_i = \frac{1}{d_i} \tag{2}$$

$$\phi_i = \frac{l_j}{\sum_{j=0}^N l_j} \tag{3}$$

Here ϕ_i is the probability that the link will be selected. We then create a cumulative probability sequence by summing the ϕ_i .

$$c_i = \sum_{i=0}^{n} \phi_i \tag{4}$$

To simulate flooded links, we randomly generate a number between [0, 1] and check into which interval it falls. The larger the c_i is, the greater the likelihood of link inundation (i.e., link removal). Through multiple runs of simulations, we can obtain a sequence of flooded links

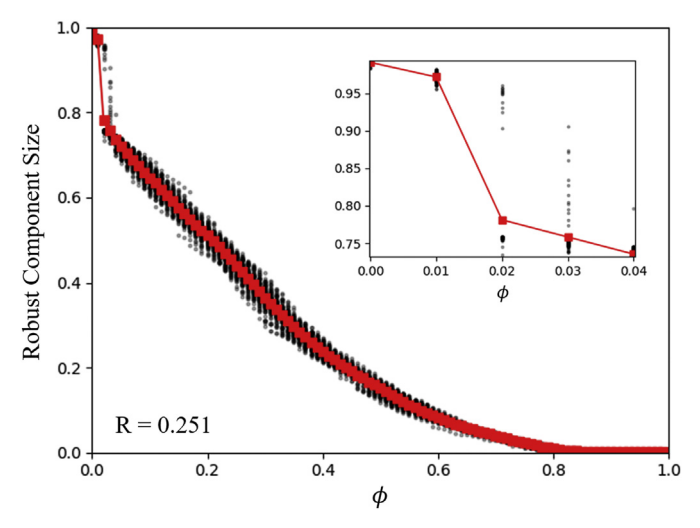


Fig. 4. Percolation process of robust component size.

and investigate the network behavior under the simulated flooding scenario. Although real-life flooding is determined by other factors such as location, land cover, and rainfall magnitude, our simplifying assumption (i.e., road inundation risk is a function of distance to floodways) enables us to approximate road inundations and to model flood propagation across the entire network to inform future infrastructure development and hazard mitigation actions. To evaluate various flooding scenarios, we use a Monte Carlo-based approach. In this study, 100 simulation runs representing different flood scenarios are generated through the aforementioned procedure, and the average network performance (robust component) is calculated.

4.3. Disrupted network access to healthcare facilities

In this paper, we mainly focus on investigating network robustness by assessing a community's post-flooding access to the healthcare facility (hospital). Denoting the flood inundation scale as ϕ (the proportion of the links inundated), Fig. 4 presents the percolation process of network robustness, measured by robust component, as the flood inundation scale increases. In this experiment, ϕ increases by 0.01 at each step. As shown in the figure, the network robustness shows a sudden drop (from 1.0 to 0.8) as ϕ increases to 0.02. This suggests that when a county-wide flooding event occurs, if 2% of the roads (4077 links) are inundated, this will result in 22% the network losing access to the healthcare facilities. One plausible explanation is that the nearfloodway roads are normally bridges or ramps that connect the major arterial to the bridge. They are critical links that connect different sections of the network together. Once these roadways inundated, the network becomes fragmented into small isolated components. If the component does not contain a healthcare facility, the whole neighborhood will lose its access to health care services. This finding urges the protection of bridges and roads in the vicinity of floodway through bridge retrofitting or road elevation. As flood propagation progress, the network's access to healthcare facilities continues to drop. When 80% of the roads are inundated, robustness will reach a critical threshold of $\phi_c = 0.8$, and whole network will lose access to healthcare facilities. Although such large scale flooding is unlikely to happen, the result allowed us to understand the intrinsic road network robustness based on its topology and location of healthcare facilities. The critical threshold ϕ_c marks the critical fraction of links/nodes whose removal will result in the complete isolation of network (Iyer et al., 2013; Vespignani, 2010). However, this measure does not capture the network behavior prior to the total collapse; therefore, inspired by Schneider et al. (2011), we used the robustness index R as in Eq. (5) to systematically measure the network robustness throughout the percolation process.

$$R = \sum_{\phi=0}^{N} rcs(\phi) \tag{5}$$

where N is the number of the incremental steps of ϕ , and $rcs(\phi)$ is the fraction of nodes in the robust component after removing a ϕ fraction of nodes. The percolation process measured by the robust component showed a total robustness of R=0.251. Comparing its upper bound value 0.5, the result indicated that the roadway network is highly vulnerable in terms of providing access to the healthcare facilities during flooding events.

Investigating the gradual flooding propagation is critical in pinpointing the damages in different scales and to understand the pressing risk of losing access to healthcare during a flooding event. As vulnerability to flooding varies from community to community and is dependent on the availability of healthcare facilities resources and exposure to flood hazards, equally important is to locate vulnerable communities for which to provide targeted protections. Therefore, in addition to the simulation of fluvial flooding due to overflow of floodways, we also examined flooding caused by Harvey. The Hurricane Harvey flood information is obtained from the Harris County flood warning system (HCFCD, 2019). The available data did not include details regarding flood depth on roads. Hence, the analysis did not consider the depth of the flood. In doing so, we assumed that a road is impassible once it is flooded (regardless of flood depth). This limitation could be addressed in future studies when more fine-grained data regarding flood depth on roads are available Employing the link removal based on the floodplain presented in Fig. 2, we first removed the links based on their likelihood for fluvial flooding based on Eq. (3). Each node's access to the healthcare facility was then calculated based on the proposed robust component and finally aggregated based on the census tract.

As shown in Fig. 2, Hurricane Harvey brought flooding mainly around the floodways. During Hurricane Harvey, the operator made the difficult decision to open the spillways of aging Barker and Addicks Dams in northwest Houston to prevent rising water in the lake from breaching the dam. Although the release of flood-water to downstream neighborhoods causing inundation of > 9000 houses (almost all of which did not have flood insurance) for more than two weeks, the decision prevented even worse destruction. We can see that Addicks and Barker Reservoir, west of Addicks, and Memorial & Briar Forest area are heavily flooded. Comparing Figs. 2 and 5, we can see that Aldine, Mount Houston, East Houston, and Channelview suffered from flood inundation. Although these areas did not experience extensive flooding, they are at very high vulnerability of losing access to healthcare facilities. This is because the flooding in the region produces a loop that isolated these communities. This finding implies that the topology and properties of infrastructure networks cause flood risk to propagate outside floodplains, a type of vulnerability not well studied due to location outside the floodplain. The Bellaire area is surrounded by many healthcare facilities; nevertheless, due to the flooding, it is vulnerable to disrupted access to the healthcare facilities. Conversely, Jacinto City, Galena Park, and Harrisburg/Manchester experienced moderate flooding; however, their vulnerability to losing hospital access is low because they are not secluded from the rest of the network. Although longer travel distance is expected, residents of these areas can still find a path to access the healthcare facility.

It should be noted that we assumed all residents would seek healthcare services within Harris County; however, communities located on the periphery of the county might have access to healthcare facilities in the adjacent counties. This could be one reason for explaining the extent of vulnerability areas, most of which showed significant vulnerability to the loss of access to healthcare facilities due to the flooding disruption. Nevertheless, the results are still valid since the adjacent counties might also be affected by flooding, and their

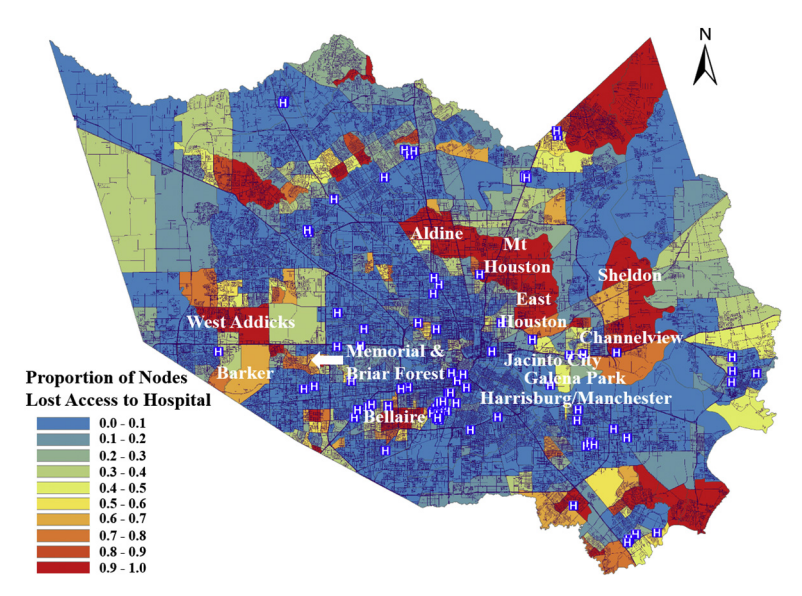


Fig. 5. Disrupted access to healthcare facilities in Harris County.

healthcare facilities may not have the capacity to serve the needs of affected populations from Harris County, who lost access to local healthcare facilities.

To identify the spatial correlation of vulnerability at the urban scale, we used Local Indicators of Spatial Association (LISA) method to identify the spatial clusters and adopted Global Moran's I test to examine the similarity and dissimilarity of the neighboring spatial units (Robinson & Quinn, 2018; Wang & Mu, 2018). Moran's I scatter plot classifies the spatial association into four quadrants of high-high, low-low, high-low, and low-high, where high-high cluster indicates a vulnerable area is surrounded by similarly high vulnerability areas. A high-low cluster indicates a vulnerable area is surrounded by low vulnerability areas, and vice versa. Fig. 6 presents the identified clusters. Moran's I test in Fig. 6(a) shows a value of 0.573 with a *p*-value of

0.001. This statistically significant clustering result suggests the existence of a homogeneous spatial pattern where regions with similar vulnerability characteristics cluster together. This spatial pattern is an emergent property arising from the characteristics of road networks and healthcare facilities. Fig. 6(b) shows that the distance decay function indicating the spatial correlation effect diminishes at the radius of 9 miles. This result suggests that the spatial reach of physical vulnerability for each area in terms of access to critical health care facilities is 9 miles in the study region. The spatial reach of physical vulnerability indicates the extent to which access disruption cascades into neighboring areas. Fig. 6(c) also shows the identified hotspots and cold spots of the physically vulnerable communities. For example, confirming the results in Fig. 5, we can see vulnerable neighborhoods that are surrounded by similarly highly vulnerable neighborhoods (101 census

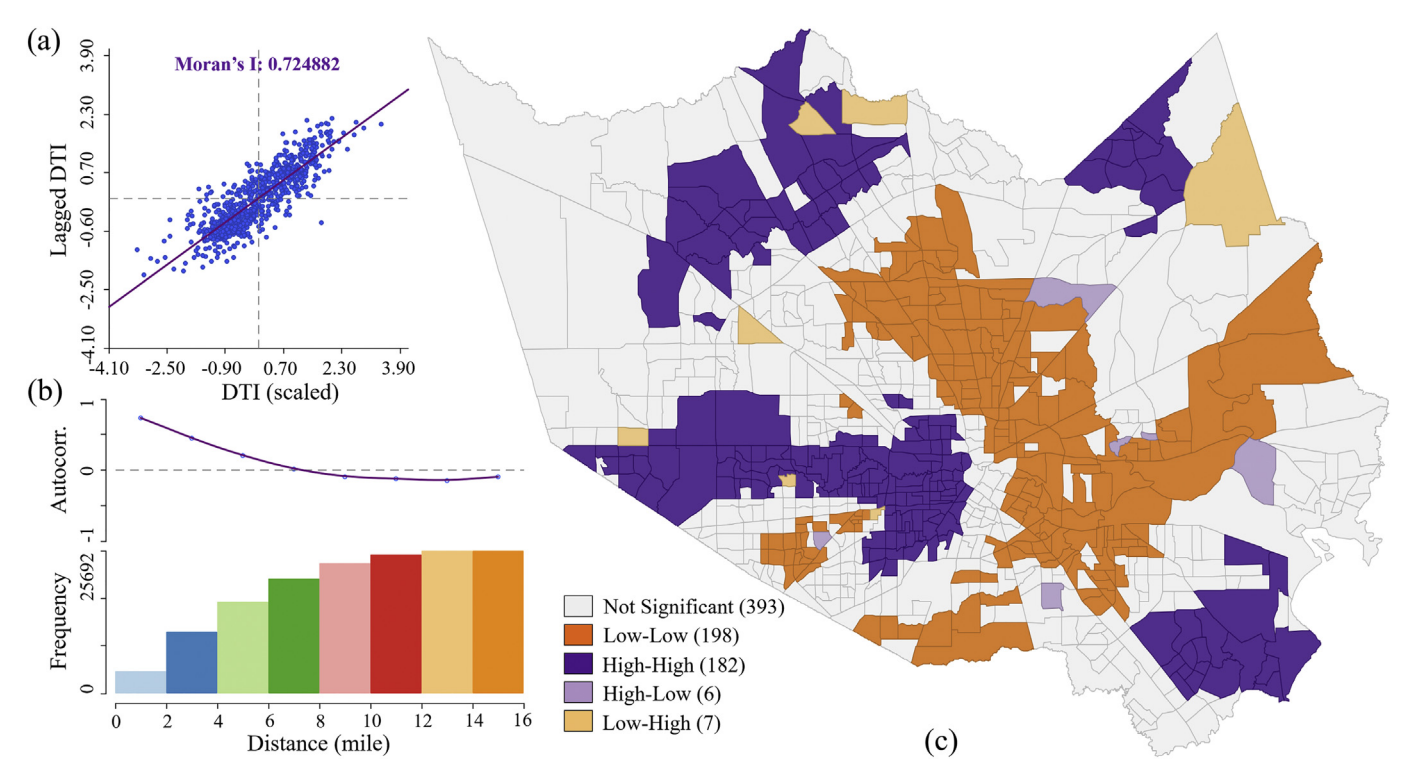


Fig. 6. Spatial cluster of physically vulnerable region facing healthcare service loss during Hurricane Harvey in Harris County.

tract) in Addicks, Aldine, Mount Houston, Sheldon, and Channelview areas. Examining low-high clusters where neighborhoods of low physical vulnerability are surrounded by high physical vulnerability reveals that these neighbors are farther from floodways; also they are either adjacent to a healthcare facility or have major transportation routes such as US-90 and I-45 that connects to a healthcare facility in other regions. In other words, the low-high areas have a unique redundancy feature that distinguishes them from their neighboring spatial areas.

5. Tolerance analysis towards disrupted access to healthcare facilities

The societal dimensions of the disrupted access to healthcare facilities can be examined based on two measures: experienced hardship and tolerance level. A self-reported level of hardship experienced by a household due to disrupted access to healthcare facilities provides an indicator of societal impacts. The level of hardship is a function of the extent of disruptions (physical infrastructure vulnerability), as well as the capability of a household to cope with disruptions. In this study, we characterize the capability to withstand disruptions as a tolerance level. Households' needs and dependence on infrastructure services vary; hence, the same level of disrupted service would impact households differently depending upon their tolerance level. The level of tolerance is shaped by two service thresholds: (1) acceptable service level, which is defined by people's need from infrastructure services in their daily lives, and (2) minimum adequate service level that a household could tolerate in a disaster setting. Households' level of tolerance is largely determined by their sociodemographic characteristics and resources available to cope with the negative impacts of service disruptions (Esmalian, Dong, et al., 2019).

5.1. Post-hurricane Harvey household survey

To examine the influence of social factors on the level of tolerance of households, a survey was designed and distributed across Harris County in the aftermath of Hurricane Harvey. The survey included questions about household socio-demographic attributes, service disruptions experienced during Harvey, hardship experienced due to service disruptions, and their level of tolerance. Households were surveyed to determine hardship experienced due to disruptions in access to healthcare facilities. Answers ranged from none at all (=1) to a great deal (=5). A households' tolerance level to service disruptions was determined by asking the respondents how many days they would be capable of tolerating loss of access to the service in the face of another natural disaster like Hurricane Harvey. An online survey panel service, Qualtrics, collected data from a sample population of the public older than 18 years of age in Harris County. The subjects were recruited by Qualtrics from different ZIP codes. Qualtrics is a private U.S. company with expertise in online data collection. Qualtrics data collection services are used by academic institutions in the United States. The survey focused on households which sheltered in place during Harvey. We included a question about evacuation and excluded responses of those who evacuated before or during Harvey. The survey was first deployed for the soft launch with 47 responses before the full data collection to ensure that the questions were clear and understandable. In total, 2242 responses were collected from all 140 ZIP codes in Harris County. After removing incomplete responses and those who finished the survey early, a sample of 1078 responses was obtained. The collected survey data well represent the demographic information of Harris County (compared with Census data). In addition, the responses cover every zip code in Harris County. Lindell and Hwang (2008) showed that using a diverse sample size for testing relationships in the model is more important than having a sample exactly representing the population. Therefore, the 1078 responses collected and the diversity encapsulated in the demographic information of the respondents are good representations of Harris County. Table 1 shows the summarized

Table 1Demographic information of survey respondents.

Variables	Categories	Frequency	Percentage (%	
Age ^a	< 2 years	69	4.13	
	2-10 years	200	11.97	
	11–17 years	211	12.63	
	18-64 years	842	50.39	
	65 years or older	349	20.88	
Education	Less than high school	23	2.13	
	High school graduate or GED	144	13.36	
	Trade/ technical vocational training	51	4.73	
	Some college	191	17.72	
	2-year degree	96	8.91	
	4-year degree	332	30.80	
	Post Graduate level	235	21.80	
	Other	6	0.56	
Income	Less than \$25,000	160	14.84	
	\$25,000-\$49,999	232	21.52	
	\$50,000-\$74,999	241	22.36	
	\$75,000-\$99,999	145	13.45	
	\$100,000-\$124,999	94	8.72	
	\$125,000-\$149,999	78	7.24	
	More than \$150,000	128	11.87	
Ethnic identity	White	641	59.46	
	Hispanic or Latino	128	11.87	
	Black or African American	208	19.29	
	American Indian or Alaska Native	8	0.74	
	Asian	40	3.71	
	Native Hawaiian or Pacific Islander	3	0.28	
	Other	50	4.64	
Resident type	Single family home	796	73.84	
	Multiple units	236	21.89	
	Mobile homes	21	1.94	
	Other	25	2.32	
Difficulty in	Yes	135	12.52	
mobility	No	943	87.48	
Disability	Yes	197	18.27	
	No	881	81.73	
No vehicle	Yes	37	3.43	
	No	1041	96.57	

^a Number of housesholds with at least one resident in the category.

demographic information in the survey.

5.2. Household's experienced hardship

Responses to the question of whether household members needed treatment at a healthcare facility during or after Hurricane Harvey (Yes = 1, No = 2) were used to assess their need for health care services. If the answer to the question was yes, respondents were asked if they had experienced inaccessibility to healthcare services because of Hurricane Harvey (Yes = 1, No = 2). In addition, households experienced hardship from losing access to healthcare facility was measured by asking the respondent to select the extent of overall hardship level that their household had experienced due to disruption of access to healthcare services, ranging from scale of none at all (=1) to a great deal (=5). Of 1078 collected responses, 111 responses mentioned that they needed healthcare services during the disastrous event. The experienced hardship of the respondents from the disruption of healthcare services was investigated using the sample data of those who had experienced the disruption. The main reason for using this subset of data was that people who did not have a need for the service would not experience any hardship. Of 111 respondents who needed access to the healthcare facility, 72 (65%) mentioned that they did not have access to healthcare due to disrupted access caused by Hurricane Harvey. The high proportion of the respondents without having access to goodquality healthcare services reported that they experienced significant hardship due to disruption. The extent of hardship that households

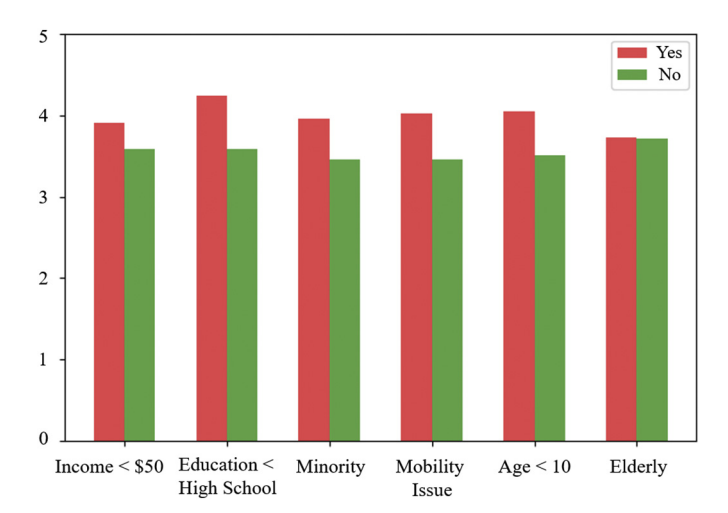


Fig. 7. Hardship disparity in loss of healthcare services.

experience due to access disruption is a combined result of disrupted access and lower tolerance to the access disruptions. Physical vulnerability and spatial patterns of disrupted access to healthcare facilities are affected by many factors, such as city planning history and urban development patterns. In this paper, we mainly focus on creating an integrated methodology for specifying and analyzing spatial patterns of risks due to disrupted access to healthcare facilities during a flooding event.

Hardship from the disruptions in healthcare accessibility was experienced disproportionately by different sub-populations. Fig. 7 shows that the experienced hardship was greater for lower-income families, racial minority groups, households with the highest education level less than or equal to high school diploma, households with mobility issues, and households with a child < 10 years of age. t-test analysis for comparing the mean hardship scores revealed that the scores are not equal at 5% level of confidence for race, education, mobility, and age < 10 years. Interestingly, there were no observed differences in the experienced hardship of older adults from the healthcare service disruptions. This could be explained by the fact that older adults have more previous disaster strike experiences and they are more prepared when a hazard warning is issued. The latent causal relationship between socio-demographic characteristics and household access to healthcare facilities (e.g., less developed region has fewer healthcare facilities, or marginalized households have poor health condition) is not within the scope of the study presented in this paper.

The variations in the level of hardship experienced were partly due to a household's levels of tolerance. The disproportionate hardship highlights that the disrupted access to healthcare services does not affect the households equally. Socially vulnerable populations experience higher hardship from these disruptions. To capture the variation in the level of tolerance, we propose an infrastructure disruption tolerance index. The DTI is a function of socio-demographic attributes of a household which vary for different infrastructure services. Unlike the general social vulnerability indices, DTI is infrastructure-specific and distinguishes the needs and coping capabilities of vulnerable sub-populations for service disruptions.

5.3. Infrastructure disruption tolerance index

Fig. 8 summarizes the process for developing the DTI related to disrupted access to healthcare facilities. We first identified the sociodemographic variables associated with the households ability to tolerate the healthcare service disruptions. Based on the survey data, we conducted a correlation analysis; results are presented in Table 2. Income, education, racial minority, family with a child < 10 years old are all correlated with tolerance to the healthcare service disruption. These

groups of people have significantly lower tolerability to such service disruptions and are in high need of assistance during a disruptive event. This study is conducted at the household-level and the specific characteristics of the individuals, such as gender, are not investigated here. Having elderly in the household is also associated with the zone of tolerance to healthcare facilities access; however, this group has expressed having a higher tolerance to service disruptions. Finally, poor access to healthcare facilities may be related to the inability to afford transportation. Hence, having no vehicle was added to the influential factors affecting, although its association with the zone of tolerance was not statistically significant at 0.01 level. These households would experience great difficulty when facing inaccessibility to healthcare services, as public transportation may be disrupted as well.

5.3.1. Influential social factors identification

In the second step, we used the identified influential factors to calculate DTI for each census tract. Based on the selected influential factors, corresponding data were extracted. For each identified influential social factor, the corresponding data entry containing a 5-year estimate of American Survey Community was extracted from the US Census Bureau for 798 census tracts in Harris County.

5.3.2. DTI generation using principal component analysis

Multiple factors affect households' tolerance to disrupted access to healthcare facilities, as shown in Table 3. Simple aggregation of these factors would neglect the intercorrelation between them and result in an unreliable DTI. To avoid this issue, we conducted a PCA to ensure the variables included are independent of each other (Lloyd, 2010). To perform PCA, all six variables were normalized to a standard scale to enable comparison of variables in different scales and different measurement units. Accordingly, variables were transformed into a common scale with mean equals 0, and standard deviation equals 1. Then, PCA was implemented, and eigenvalues for principal components were calculated. Based on the proportion of the variance explained, three principal components (PC1, PC2, and PC3) with the highest eigenvalues were considered for further analysis. These three components explain 82% of the variance in the data. Therefore, they can properly encapsulate the effect of social factors affecting the community's tolerance to loss of access to healthcare facilities. Scree plot in Fig. 9 shows the percentage of variance explained by each principal component. The DTI was then calculated by summing up weighted values of three principal components for each census tract. The percentage of variance explained by each principal component was considered as the weight of the component.

$$DTI_k = \sum_{i=1}^{3} \lambda_i \times y_i \tag{6}$$

where λ_i is the proportion of variance explained by the components, and y_i is the component scores. To convert the DTI into a comparable scale, we scale the calculated DTI to the range of [0, 1].

$$DTI_{k(\text{scaled})} = \frac{DTI_k - DTI_{\min}}{DTI_{\max} - DTI_{\min}}$$
(7)

where $DTI_{k(scaled)}$ is the scaled disruption tolerance index for census tract k, and DTI_{min} and DTI_{max} are the minimum and maximum disruption tolerance scores for census tracts in the county calculated, respectively.

Fig. 10 shows the calculated DTI values across Harris County in the census tract scale. The DTI ranges from 0 to 1 with a mean of 0.504 and a variance of 0.149. A high DTI value indicates that the community has high tolerance to healthcare service disruption. The location-based DTI values show that areas such as Greater Uptown, River Oaks, Upper Kirby Area, and Bellaire have a greater tolerance, and communities such as Aldine, Sheldon, and Channelview have a lower tolerance to losing access to healthcare facilities. For example, the average DTI for

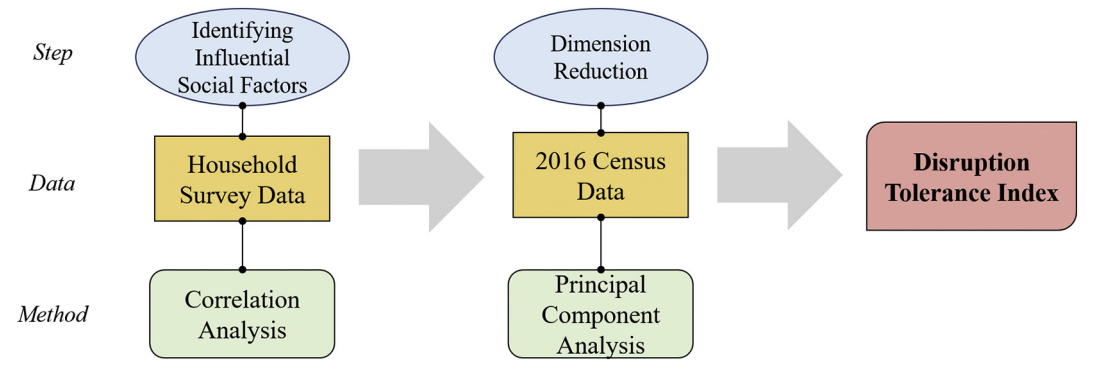


Fig. 8. Procedure to develop disruption tolerance index.

River Oaks is 0.899, while Aldine community has an average DTI of 0.132. As we dive into the sociodemographic characteristics, we can see the average income in the River Oaks community is 149,669 USD, with only 2% of the population over 25 without school degree while Aldine has an average income of 12,618 USD with 59% the population over 25 without school degree. As suggested in the survey and literature, high income and education levels are associated with the high tolerance of households in facing inaccessibility to healthcare facilities. Therefore, we can expect that such a significant disparity in income contributes to the difference in tolerance to disrupted access to healthcare facilities in these two communities. The other contributing factor of the high tolerance to the access disruption to healthcare facilities in River Oaks community is the low percentage of the minority population. Literature and survey have been emphasizing that the minority population is more socially vulnerable and have lower tolerance to access disruption to services. Therefore, Aldine, with an average of 90.8% minority population is more vulnerable to loss of access to healthcare service compare to the River Oaks, where only 19.2% of minorities. The poor access to healthcare facilities may be also related to the inability to afford personal vehicles as wealthier households do. Besides, flooding also impacts the operation of public transportation; this also partially explains why vulnerable households have trouble accessing healthcare services.

Based on a spatial analysis of the derived DTI map, we unveil the spatial pattern embedded in the tolerance to disrupted access to healthcare facilities. Fig. 11(a) shows a highly positive Moran's I value of 0.725, which indicates there is a strong correlation among spatial areas in terms of their population's tolerance to healthcare service disruption. Fig. 11(b) shows a critical threshold of 7 miles for spatial autocorrelation. This result suggests that when the distance between two areas exceeds 7 miles, their similarity of DTI decays. In other words, the spatial dependence of a sub-population's tolerance to access disruption to healthcare facilities is contained within the region. Fig. 11(c) also shows the identified spatial clusters of hot – /cold-spots for DTI. The high-high cluster represents neighborhoods with high DTI that are surrounded by neighborhoods with similarly high DTI and vice versa. In areas where both the physical and social vulnerability to the disruptions are high, there is a spatial mismatch (Kain, 1992). In these vulnerable areas, the co-existence of the physical and social vulnerability signifies the impact on the residents and creates many

Table 3Correlation between selected influential social factors.

	Income	Education	Elderly	Minority	No vehicle	Children
Income Education Elderly Minority No Vehicle Children	1 -0.67** 0.06 -0.79** -0.37** -0.45**	1 -0.08 0.77** 0.41** 0.49**	1 -0.13** 0.00 -0.18**	1 0.49** 0.45**	1 0.25**	1

^{*, **} Results are significant at 0.01, 0.001 confidence level, respectively.

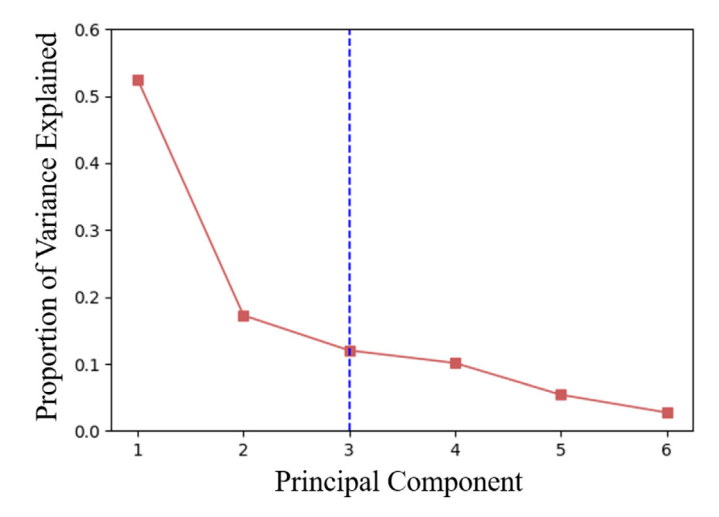


Fig. 9. Proportion of the variance explained by each principal component.

difficulties for the affected households. Households with a low ability to tolerate the disruptions are located in areas with a high vulnerability to access disruptions to healthcare facilities. From the identified cluster, we can observe that neighborhoods along the Buffalo Bayou, northwest and southeast of Harris County have high tolerance to loss of access to healthcare facilities during flooding, while neighborhoods in Greens Bayou and along the US-90 corridor have low tolerance. More hospitals are located in the high-high clusters than in the low-low areas. We also

Table 2Correlation results for identifying the influential social factors.

Factors	Spearman correlation analysis									
	Income	Education	Minority	Mobility	Disability	Elderly	Age < 10	Mobile home	Multiple unit	No vehicle
Zone of tolerance Correlation coefficient Significance	0.169 0.000*	0.125 0.000*	-0.149 0.000*	0.039 0.201	0.028 0.356	0.095 0.002*	-0.124 0.000**	-0.069 0.024	-0.065 0.034	- 0.056 0.065

^{*, **} Results are significant at 0.01, 0.001 confidence level, respectively.

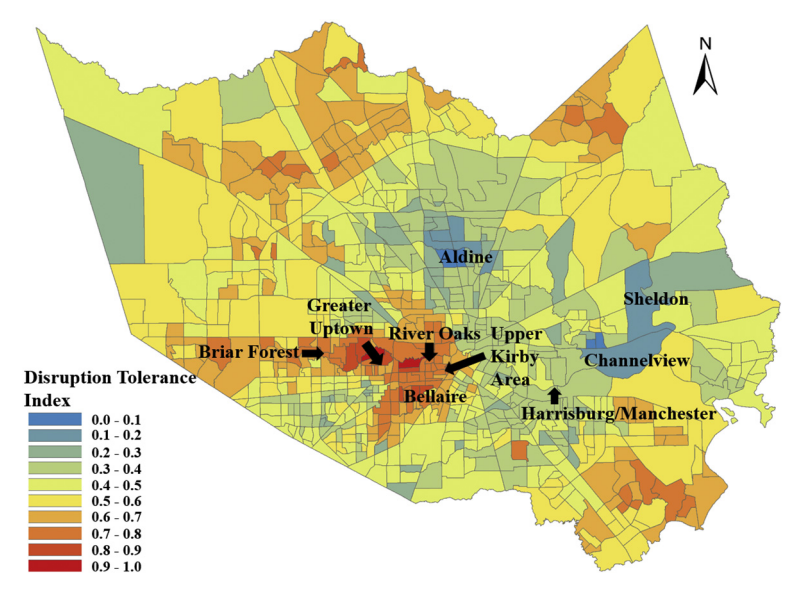


Fig. 10. Disruption tolerance index mapping of Harris County in census tract scale.

observed that only a few high-low clusters where high tolerance communities are adjacent to low tolerance communities. The results confirm the existence of distinct spatial clusters with homogeneous level of tolerance to disrupted access to healthcare facilities.

6. Integrated physical-social community vulnerability

Community vulnerability to disasters is determined not only by the physical vulnerability caused by the surrounding infrastructure failure risk but also the capability of people to cope with infrastructure disruption. Here, we consider a high tolerance for access disruption to healthcare facilities as a sign of lower social vulnerability. Therefore, social vulnerability is represented by the converse of DTI. To provide a holistic assessment of community vulnerability in facing disrupted

access to healthcare facilities, we link both simulated physical vulnerability caused by disrupted access to healthcare facilities during floods and the corresponding DTI together to enable an integrated vulnerability assessment through an integrated spatial analysis. The Bivariate Local Moran's I method is employed to investigate the spatial correlation where both physical and social vulnerabilities are considered. The integrated physical-social community vulnerability spatial analysis enables the identification of vulnerability origin in each community, which provides invaluable insights on devising proper plans and policies in reducing future hazard risks. Not only will the identified causes of vulnerability prioritize the targeted hazard risk reduction, but they also inform the decision-makers regarding the proper types of policy for each community.

Fig. 12 presents the spatial correlation of physical and social

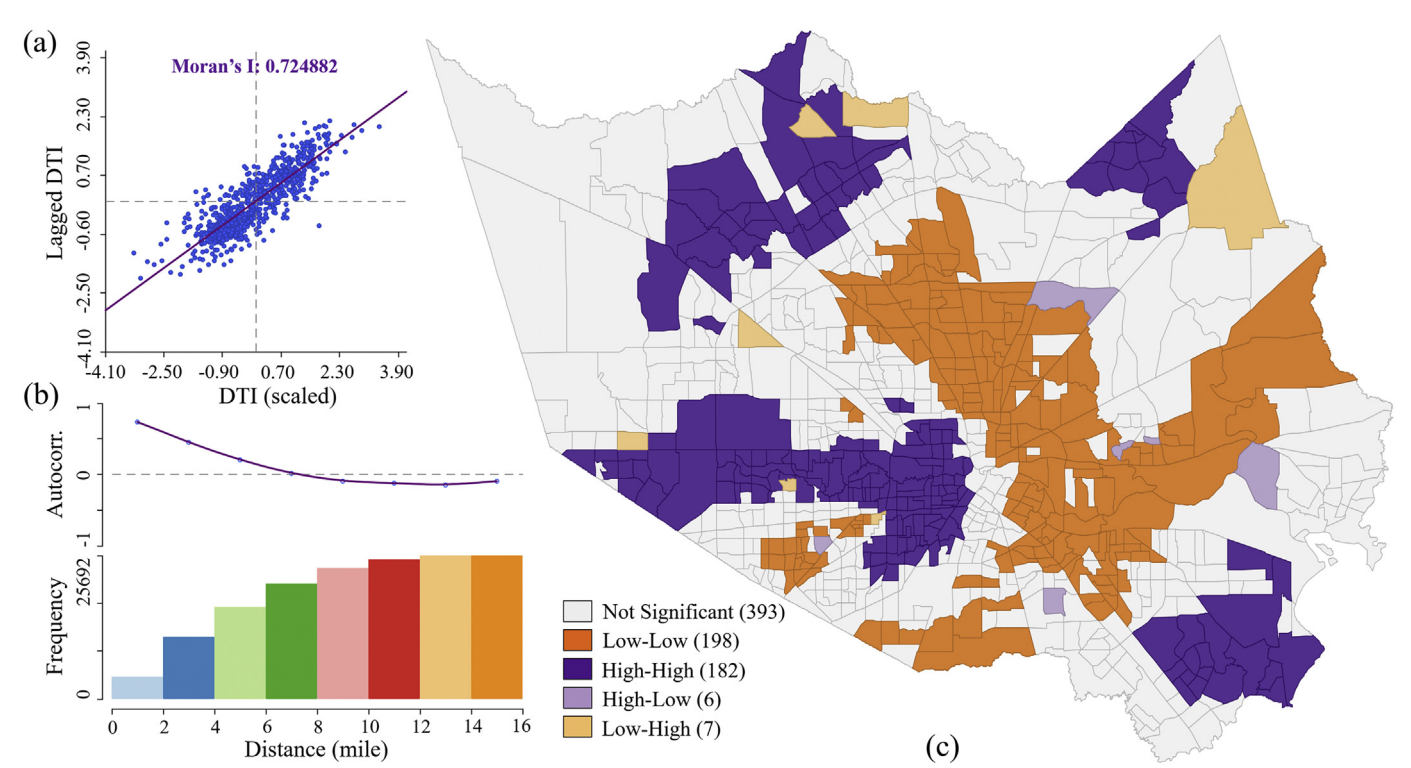


Fig. 11. Spatial cluster of DTI to disrupted access to healthcare facilities in Harris County.

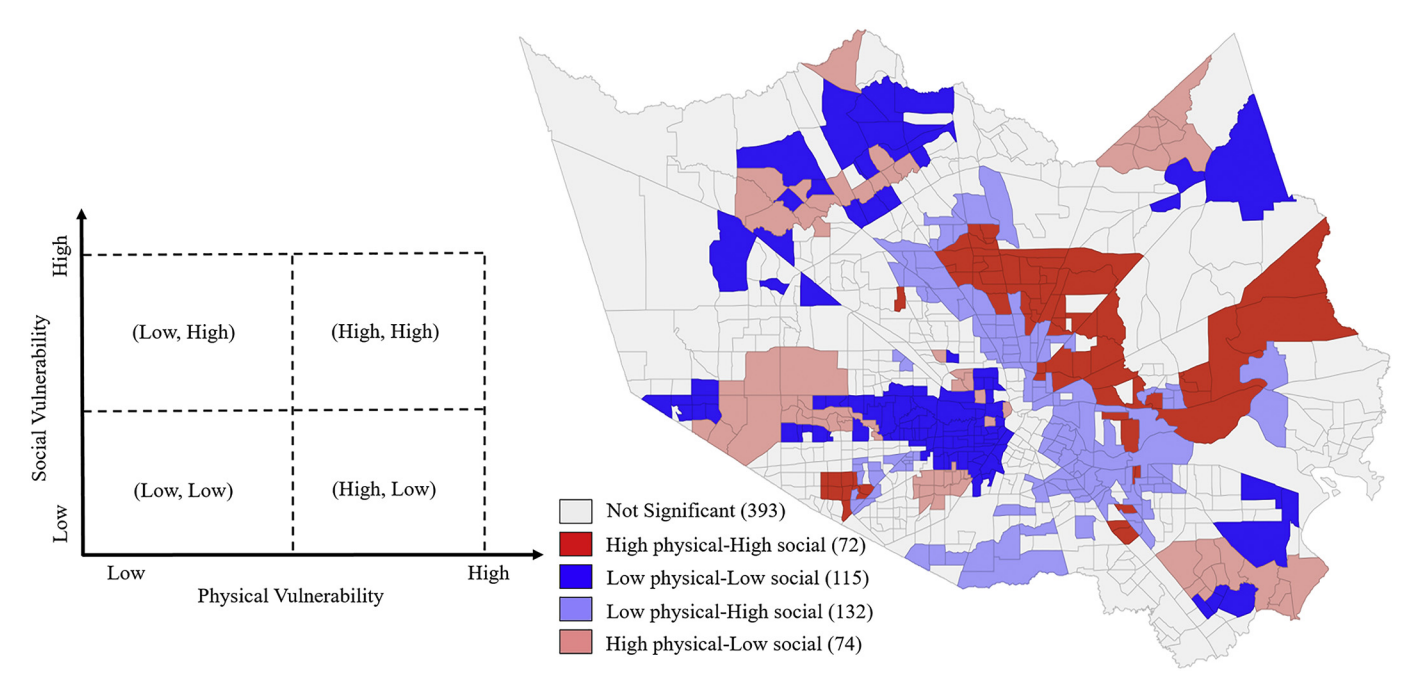


Fig. 12. Integrated physical-social communities vulnerability assessment.

vulnerability. High physical - high social cluster indicates that the identified areas are not only highly prone to loss of access to healthcare facilities during flooding but also have a low tolerance to access disruption to healthcare services. Spatial co-existence of physical vulnerability and low tolerance to service disruption (i.e., high social vulnerability) was observed by implementing the proposed framework in Harris County. In these areas, residents with a low tolerance to the access disruptions to healthcare facilities were located in areas that are highly physically vulnerable to access disruption to healthcare facilities. Two primary reasons could explain this spatial co-location of physical vulnerability and low tolerance to disrupted access to healthcare facilities. First, due to the limited political access (Cutter et al., 2003), these groups live in areas that are exposed to high flood risk with poor infrastructure conditions. In these areas, the recurring flooding adds to the impacts on the physical infrastructure and leads to severe damage when facing flooding. Second, the marginalized groups in these areas have fewer resources, such as power backups, to withstand the impacts of the disruptions on their well-being. Moreover, these households might have a poorer health condition (Aday, 1994; Shinn, Knickman, & Weitzman, 1991) and, therefore, need more medical attention. The household's greater need for healthcare also decreases their tolerance to the access disruptions (Esmalian, Dong, et al., 2019). Thus, in these areas being a marginalized group would indirectly cause a higher hardship on the households. From the policy-making perspective, such vulnerable neighborhood clusters are in the highest priority for investment in hazard mitigation and emergency response planning in terms of prioritizing the infrastructure protections and investing in critical resources to ensure the availability of healthcare services in these communities. In the case of Harris County (Fig. 12), 72 census tracts in Aldine, Sheldon, and Channelview area are both physically and socially vulnerable to the disruption of access to healthcare facilities. These neighborhoods mainly located in the south and center of the county, where the number of healthcare facilities is relatively low, but the location is in the vicinity of flood-prone areas. These neighborhoods require targeted protection on the existing facilities and consideration of new facility development. The fact that these neighborhoods are both physically and socially vulnerable necessitates open dialogue and collaborative planning between different actors that are involved in the policy-making. On the other hand, low physical - low social clusters, such as east of downtown Houston, northwest and

northeast Harris County show low vulnerability to access disruption to healthcare services. Looking at the critical facilities distribution and sociodemographic characteristics, we can see that many healthcare facilities are densely located in this region and residents are highly educated with very high income.

High physical - low social clusters such as east (Briar Forest, Addicks and Barker reservoir), southeast (Galveston Bay), and northeast (San Jacinto River) Harris County are highly vulnerable to flood disruption of healthcare access to hospitals since they are closely located to 100year and 500-year floodplains. In this case, infrastructure improvement policies can be devised such as (1) road elevation to minimize the risk of road inundation and (2) stormwater drainage network enhancement to increase the discharge capacity of the flood control system, which reduces the risk of inundation both for facilities and road segments. In addition, the continuous growth of population and economic assets in flood-prone areas makes these communities even more vulnerable to flooding (Aerts et al., 2018; Jongman, Ward, & Aerts, 2012). Although communities in these affluent developed areas are more resourceful to cope with the access disruption to healthcare facilities; future infrastructure developments should be minimized in these areas to avoid flood risk escalation.

Regarding low physical - high social vulnerability clusters are closely located along the I-45, I-610, and US-90 corridor, these communities are at low risk of losing access to the healthcare facilities in the event of flooding as they either have healthcare facilities within the community, or they have easier access to the route that connects to healthcare facilities in other regions. These regions, however, have a low tolerance to the disruption of access to healthcare facilities. Although they have a low risk of physical disruption, due to the unpredictable nature of the flooding events, flood events like Hurricane Harvey could lead to a catastrophic impact on these communities. Proper actions for these neighborhoods can focus on implementing programs to increase the households awareness of flooding risk and knowledge of proper protective actions to take in case of disruptions. In addition, emergency response plans could account for the low tolerance of these areas to disrupted access to healthcare facilities.

7. Discussion

The spatial analysis in this study was conducted at the census tract

level. Using tract-level data for vulnerability analysis provides great insights on policy-making as it allows policymakers to identify vulnerable hotspots and coldspots and implement policies to mitigate the impacts of future hazardous events. Moreover, the clustering of the physical and social vulnerability highlights that the vulnerability of the areas is not randomly distributed throughout the area, but the neighboring areas which have similar attributes. Using tract data, however, may influence the results of the spatial analysis due to the data aggregation in geographic boundaries, which is known as the modifiable areal unit problem (MAUP) (Jelinski & Wu, 1996; Parenteau & Sawada, 2011). However, due to the availability of census data at the tract level, the spatial analysis is not tested in other spatial scales or zonings.

Planning and urban history can also contribute to the existing vulnerability. Houston is the only city without zoning policies in North America and is well known for its modest land-use regulations. Growing urbanization with dense development in Houston is, however, not parallelized with an equivalent focus on hazard mitigation infrastructure investment. This conflict among the rapid urban development and poor urban planning, as well as underinvestment in flood control infrastructure systems, is one of the reasons that Houston remains as one of the most flood-prone cities in the nation. Understanding the causal effect between the planning history and the current state of vulnerability is of great help to identify the planning decisions that have contributed to the vulnerability of different areas in the city. Different aspects considered in the proposed integrated physical-social vulnerability assessment framework can be a representative of the planning impacts on the current configuration of vulnerability. For example, the growth of urban areas is often concentrated in the areas located close to rivers and waterways (Aerts et al., 2018) and it can make such areas more vulnerable. This has been considered in the process of physical vulnerability quantification by modeling road inundation as a function of closeness to the waterway, which indirectly captures the impact of the development pattern on the vulnerability of urban areas. Besides, the emergence of clusters with high physical- high social vulnerability in the integrated spatial analysis captures whether the existing attempts for city development and hazard mitigation were able to account for vulnerable populations and provide them with more robust accessibility. Meanwhile, the formation of urban areas with high physical high social vulnerability indicates that the planning practices and current policy settings have neglected the urgency of planning for vulnerability reduction in socially vulnerable regions, which consequently led to the clustering of urban areas that are vulnerable both physically and socially. In contrast, the formation of clusters that are neither physically nor socially vulnerable shows that the state of planning in the city is dedicating more resources to the urban areas that are less socially vulnerable.

The proposed integrated physical-social community vulnerability framework can be also transferred to other locations and scenarios. Given the city network topology (e.g., transportation) and critical facility locations (e.g., fire station, grocery store, gas station), the proposed percolation simulation can assess the network's physical vulnerability in terms of accessing different infrastructure services in the face of various disaster disruptions, such as earthquake (Dong, Mostafizi, Wang, & Bosa, 2016) and tsunami (Mostafizi, Wang, Cox, Cramer, & Dong, 2017; Mostafizi, Wang, Cox, & Dong, 2019). In addition, households' experienced hardship and sociodemographic characteristics can be collected through a household survey. The proposed framework enables a better understanding of the network vulnerability and facilitates the decision-makers to (1) identify critical communities for road retrofitting and protection in order to improve their access to critical facilities during flood, (2) examine the sitting of existing hospital for relocation and location for future healthcare facilities to reduce the community vulnerability in flooding events, and (3) prioritize the emergency response regarding needs of healthcare service in identified hot-spot areas.

8. Conclusion

This paper contributes to the existing vulnerability assessment knowledge by presenting an integrated physical-social vulnerability analysis framework based on an assessment of the disrupted access to healthcare facilities, as well as a community's tolerance of healthcare service disruption. The proposed integrated framework enables identifying the spatial clusters and patterns of vulnerable communities to inform prioritizing the physical and social infrastructure development activities/policies.

The physical vulnerability assessment employed a probabilistic percolation approach to investigate the access loss to healthcare facilities facing fluvial flooding in Harris County, Texas. The robust component analysis reveals that 2% of near-floodway road disruption will lead to a 20% drop on network access to healthcare facilities. The access loss was then mapped to the census tracts to show the spatial distribution of physical vulnerability. The identified spatial cluster of the physical vulnerability highlights the spatial reach of access disruption to healthcare facilities is 9 miles, indicating the extent of spatial dependence. Another contribution of the proposed framework is the characterization of disruption tolerance. Since the general social vulnerability measure does not capture a sub-population group's tolerance to a particular infrastructure service disruption, a new measure, DTI, was proposed and tested to measure a community's tolerance to healthcare service disruption. Social factors including income, education, racial minority, family with a child < 10 years old, elderly, and have no vehicle are all correlated with tolerance to the healthcare service disruption. The spatial analysis of DTI identified spatial clusters whose populations have low tolerance to disrupted access to healthcare services. The spatial dependence of vulnerability indicates that there exists a homogeneous pattern where regions with similar vulnerability cluster together. Integrating the physical and social vulnerability elements through a spatial analysis, different categories of vulnerable communities are unveiled. The integrated physical-social analysis revealed the spatial pattern of vulnerability in the study region to inform hazard mitigation, emergency response planning, and infrastructure prioritization processes.

The proposed framework was tested on the publicly available data set and can thus be adapted to other cities and also different types of critical facilities such as grocery stores, gas stations, and pharmacies. In terms of study limitations, we mainly focused on fluvial flooding in conducting physical network robustness analysis; however, the urban flooding is particularly challenging due to the complex interactions of surface and underground flows. Therefore, understanding the interaction of surface flow (bayou, river, and channel) and underground flow (stormwater drainage system) and their impact on roadways is critical for accurate assessment of community flood risk. In future research, dependencies between flood control/stormwater drainage systems and transportation networks could be analyzed to present a more comprehensive characterization of the network vulnerability. Besides, with the aging of the states infrastructure systems and increasing flooding risks, the likelihood of infrastructure failure varies across the network. Therefore, the infrastructure fragility condition could be also incorporated into the disruption probability calculation to devise a more accurate infrastructure failure scheme. Understanding how city structure, planning decisions, and development patterns in history shaped the vulnerability of a city is of great importance and should be investigated in the future. In addition, in order to capture more dynamic travel behaviors in a post-flooding scenario, landscape variability (i.e., elevation) and inundation severity (i.e., inundation depth) should also be included in future research (upon the availability of data).

Acknowledgement

The authors would like to acknowledge funding support from the National Science Foundation (NSF), United States Of America, CRISP

2.0 Type 2 #1832662: "Anatomy of Coupled Human-Infrastructure Systems Resilience to Urban Flooding: Integrated Assessment of Social, Institutional, and Physical Networks" and CAREER#1846069: Household Network Modeling and Empathic Learning for Integrating Social Equality into Infrastructure Resilience Assessment. Publication supported in part by an Institutional Grant (NA18OAR4170088) to the Texas Sea Grant College Program from the National Sea Grant Office, National Oceanic and Atmospheric Administration, U.S. Department of Commerce. Any opinions, findings, and conclusions or recommendations expressed in this research are those of the authors and do not necessarily reflect the view of the funding agencies.

References

- Aday, L. A. (1994). Health status of vulnerable populations. Annual Review of Public Health, 15(1), 487–509.
- Adger, W. N., Brooks, N., Bentham, G., Agnew, M., & Eriksen, S. (2005). New indicators of vulnerability and adaptive capacity. Tyndall Centre for Climate Change Research Norwich.
- Aerts, J., Botzen, W., Clarke, K., Cutter, S., Hall, J. W., Merz, B., ... Kunreuther, H. (2018). Integrating human behaviour dynamics into flood disaster risk assessment. *Nature Climate Change*, 1.
- America, O. (2017). Hurricane Harvey and equitable recovery: Mapping social vulnerability and intensity of wind and flooding from Hurricane Harvey in Texas. https:// www.oxfamamerica.org/static/media/files/Hurricane-Harvey-Equitable-Recovery-Oxfam.pdf.
- Anderson, C. C., Hagenlocher, M., Renaud, F. G., Sebesvari, Z., Cutter, S. L., & Emrich, C. T. (2019). Comparing index-based vulnerability assessments in the Mississippi delta: Implications of contrasting theories, indicators, and aggregation methodologies. International Journal of Disaster Risk Reduction. 101128.
- ATC (2016). Critical assessment of lifeline system performance: Understanding societal needs in disaster recovery. US Department of Commerce, National Institute of Standards and Technology, Applied Technology Council.
- Bashan, A., Berezin, Y., Buldyrev, S. V., & Havlin, S. (2013). The extreme vulnerability of interdependent spatially embedded networks. *Nature Physics*, 9(10), 667.
- Beccari, B. (2016). A comparative analysis of disaster risk, vulnerability and resilience composite indicators. PLoS Currents, 8.
- Berche, B., von Ferber, C., Holovatch, T., & Holovatch, Y. (2009). Resilience of public transport networks against attacks. *The European Physical Journal B, 71*(1), 125–137.
- Berdica, K. (2002). An introduction to road vulnerability: What has been done, is done and should be done. *Transport Policy*, 9(2), 117–127.
- Berezin, Y., Bashan, A., Danziger, M. M., Li, D., & Havlin, S. (2015). Localized attacks on spatially embedded networks with dependencies. Scientific Reports, 5, 8934.
- Bevacqua, A., Yu, D., & Zhang, Y. (2018). Coastal vulnerability: Evolving concepts in understanding vulnerable people and places. Environmental Science & Policy, 82, 19–29.
- Buldyrev, S. V., Parshani, R., Paul, G., Stanley, H. E., & Havlin, S. (2010). Catastrophic cascade of failures in interdependent networks. *Nature*, 464(7291), 1025.
- Chang, S. E., & Nojima, N. (2001). Measuring post-disaster transportation system performance: The 1995 Kobe earthquake in comparative perspective. *Transportation Research Part A: Policy and Practice*, 35(6), 475–494.
- Charles, C. Z. (2003). The dynamics of racial residential segregation. Annual Review of Sociology, 29(1), 167–207.
- Chen, A., Yang, C., Kongsomsaksakul, S., & Lee, M. (2007). Network-based accessibility measures for vulnerability analysis of degradable transportation networks. *Networks and Spatial Economics*, 7(3), 241–256.
- Chen, A., Yang, H., Lo, H. K., & Tang, W. H. (2002). Capacity reliability of a road network: An assessment methodology and numerical results. *Transportation Research Part B: Methodological*, 36(3), 225–252.
- Church, R., & Scaparra, M. P. (2007). Analysis of facility systems reliability when subject to attack or a natural disaster. *Critical infrastructure* (pp. 221–241). Springer.
- Cohen, R., Havlin, S., & Ben-Avraham, D. (2003). Efficient immunization strategies for computer networks and populations. *Physical Review Letters*, 91(24), 247901.
- Coleman, N., Esmalian, A., & Mostafavi, A. (2019). Equitable resilience in infrastructure systems: Empirical assessment of disparities in hardship experiences of vulnerable populations during service disruptions. *Natural Hazards Review*.
- Crucitti, P., Latora, V., Marchiori, M., & Rapisarda, A. (2004). Error and attack tolerance of complex networks. *Physica A: Statistical Mechanics and its Applications*, 340(1), 388–394.
- Cutter, S., Emrich, C., Morath, D., & Dunning, C. (2013). Integrating social vulnerability into federal flood risk management planning. *Journal of Flood Risk Management*, 6(4), 332–344
- Cutter, S. L., Boruff, B. J., & Shirley, W. L. (2003). Social vulnerability to environmental hazards. Social Science Quarterly, 84(2), 242–261.
- Cutter, S. L., & Finch, C. (2008). Temporal and spatial changes in social vulnerability to natural hazards. Proceedings of the National Academy of Sciences, 105(7), 2301–2306.
- Dargin, J. S., & Mostafavi, A. (2019). Human-centric infrastructure resilience: Uncovering well-being risk disparity due to infrastructure disruptions in disasters. PLoS ONE.
- De Oliveira, E. L., Da Silva Portugal, L., & Junior, W. P. (2014). Determining critical links in a road network: Vulnerability and congestion indicators. *Procedia-Social and Behavioral Sciences*, 162, 158–167.

- Dehghani, M. S., Flintsch, G., & McNeil, S. (2014). Impact of road conditions and disruption uncertainties on network vulnerability. *Journal of Infrastructure Systems*, 20(3), 04014015.
- Dong, S., Mostafizi, A., Wang, H., & Bosa, P. (2016). Post-disaster mobility in disrupted transportation network: Case study of Portland, Oregon. Seventh China-Japan-US trilateral symposium on lifeline earthquake engineering. Shanghai, China: ASCE.
- Dong, S., Mostafizi, A., Wang, H., Gao, J., & Li, X. (2019). Measuring the topological robustness of transportation networks to disaster-induced failures: A percolation approach. *Journal of Infrastructure Systems*.
- Dong, S., Wang, H., Mostafavi, A., & Gao, J. (2019). Robust component: A robustness measure that incorporates access to critical facilities under disruptions. *Journal of the Royal Society Interface*, 16(157), 20190149.
- Dong, S., Wang, H., Mostafizi, A., & Song, X. (2020). A network-of-networks percolation analysis of cascading failures in spatially co-located road-sewer infrastructure networks. *Physica A: Statistical Mechanics and its Applications*, 538, 122971.
- Duan, Y., & Lu, F. (2013). Structural robustness of city road networks based on community. Computers, Environment and Urban Systems, 41, 75–87.
- Dwyer, A., Zoppou, C., Nielsen, O., Day, S., & Roberts, S. (2004). Quantifying social vulnerability: A methodology for identifying those at risk to natural hazards.
- Ellingwood, B. R., Cutler, H., Gardoni, P., Peacock, W. G., van de Lindt, J. W., & Wang, N. (2016). The Centerville virtual community: A fully integrated decision model of interacting physical and social infrastructure systems. Sustainable and Resilient Infrastructure, 1(3–4), 95–107.
- Esmalian, A., Dong, S., Coleman, M., & Mostafavi, A. (2019). Determinants of risk disparity due to infrastructure service losses in disasters: A household service gap model. *Risk Analysis*.
- Esmalian, A., Ramaswamy, M., Rasoulkhani, K., & Mostafavi, A. (2019). Agent-based modeling framework for simulation of societal impacts of infrastructure service disruptions during disasters. *Computing in civil engineering 2019: Smart cities, sustainability, and resilience* (pp. 16–23). VA: American Society of Civil Engineers Reston.
- Fatemi, F., Ardalan, A., Aguirre, B., Mansouri, N., & Mohammadfam, I. (2017). Social vulnerability indicators in disasters: Findings from a systematic review. *International Journal of Disaster Risk Reduction*, 22, 219–227.
- Flanagan, B. E., Gregory, E. W., Hallisey, E. J., Heitgerd, J. L., & Lewis, B. (2011). A social vulnerability index for disaster management. *Journal of Homeland Security and Emergency Management*. 8(1).
- Frigerio, I., & De Amicis, M. (2016). Mapping social vulnerability to natural hazards in Italy: A suitable tool for risk mitigation strategies. *Environmental Science & Policy*, 63, 187–196.
- Fuchs, S., Kuhlicke, C., & Meyer, V. (2011). Editorial for the special issue: Vulnerability to natural hazards the challenge of integration. *Natural Hazards*. 58(2), 609–619.
- Ganin, A. A., Kitsak, M., Marchese, D., Keisler, J. M., Seager, T., & Linkov, I. (2017).Resilience and efficiency in transportation networks. Science Advances, 3(12).
- Gao, J., Buldyrev, S. V., Havlin, S., & Stanley, H. E. (2011). Robustness of a network of networks. *Physical Review Letters*, 107(19), 195701.
- Grinberger, A. Y., & Felsenstein, D. (2016). Dynamic agent based simulation of welfare effects of urban disasters. Computers, Environment and Urban Systems, 59, 129–141.
- Hagenlocher, M., Renaud, F. G., Haas, S., & Sebesvari, Z. (2018). Vulnerability and risk of deltaic social-ecological systems exposed to multiple hazards. Science of the Total Environment. 631, 71–80.
- HCFCD (2019). Harris county flood control district, Harris county flood warning system. https://www.harriscountyfws.org.
- Helderop, E., & Grubesic, T. H. (2019). Streets, storm surge, and the frailty of urban transport systems: A grid-based approach for identifying informal street network connections to facilitate mobility. Transportation Research Part D: Transport and Environment.
- Holme, P., Kim, B. J., Yoon, C. N., & Han, S. K. (2002). Attack vulnerability of complex networks. *Physical Review E*, 65(5), 056109.
- Huang, X., Gao, J., Buldyrev, S. V., Havlin, S., & Stanley, H. E. (2011). Robustness of interdependent networks under targeted attack. *Physical Review E*, 83(6), 065101.
- Iyer, S., Killingback, T., Sundaram, B., & Wang, Z. (2013). Attack robustness and centrality of complex networks. PLoS One, 8(4), e59613.
- Jelinski, D. E., & Wu, J. (1996). The modifiable areal unit problem and implications for landscape ecology. *Landscape Ecology*, 11(3), 129–140.
- Jenelius, E. (2009). Network structure and travel patterns: Explaining the geographical disparities of road network vulnerability. *Journal of Transport Geography*, 17(3), 234–244.
- Jenelius, E., & Mattsson, L.-G. (2015). Road network vulnerability analysis: Conceptualization, implementation and application. *Computers, Environment and Urban Systems*, 49, 136–147.
- Jongman, B., Ward, P. J., & Aerts, J. C. (2012). Global exposure to river and coastal flooding: Long term trends and changes. Global Environmental Change, 22(4), 823–835.
- Kain, J. F. (1992). The spatial mismatch hypothesis: Three decades later. Housing Policy Debate, 3(2), 371–460.
- Khazai, B., Merz, M., Schulz, C., & Borst, D. (2013). An integrated indicator framework for spatial assessment of industrial and social vulnerability to indirect disaster losses. *Natural Hazards*, 67(2), 145–167.
- Kulkarni, R. G., Stough, R. R., & Haynes, K. E. (2000). Towards a percolation model of accessibility: An exploratory step. Computers, Environment and Urban Systems, 24(5), 421–434.
- Kwan, M.-P., & Weber, J. (2008). Scale and accessibility: Implications for the analysis of land use-travel interaction. Applied Geography, 28(2), 110–123.
- Li, D., Li, G., Kosmidis, K., Stanley, H., Bunde, A., & Havlin, S. (2011). Percolation of spatially constraint networks. EPL (Europhysics Letters), 93(6), 68004.
- Li, Q., Dong, S., & Mostafavi, A. (2019a). Modeling of inter-organizational coordination

- dynamics in resilience planning: A multilayer network simulation framework. *Computing in civil engineering 2019: Smart cities, sustainability, and resilience* (pp. 515–522). VA: American Society of Civil Engineers Reston.
- Li, Q., Dong, S., & Mostafavi, A. (2019b). Modeling of inter-organizational coordination dynamics in resilience planning of infrastructure systems: A multilayer network simulation framework. PLoS ONE, 14(11), e0224522.
- Lindell, M. K., & Hwang, S. N. (2008). Households' perceived personal risk and responses in a multihazard environment. Risk Analysis: An International Journal, 28(2), 539–556.
- Lloyd, C. D. (2010). Analyzing population characteristics using geographically weighted principal components analysis: a case study of northern ireland in 2001. Computers, Environment and Urban Systems, 34(5), 389–399.
- Martins, V. N., e Silva, D. S., & Cabral, P. (2012). Social vulnerability assessment to seismic risk using multicriteria analysis: The case study of Vila franca do campo (são Miguel island, Azores, Portugal). Natural Hazards, 62(2), 385–404.
- Mattsson, L.-G., & Jenelius, E. (2015). Vulnerability and resilience of transport systems—a discussion of recent research. Transportation Research Part A: Policy and Practice, 81, 16–34.
- Mayaud, J. R., Tran, M., Pereira, R. H., & Nuttall, R. (2019). Future access to essential services in a growing smart city: The case of surrey, British Columbia. Computers, Environment and Urban Systems, 73, 1–15.
- Mostafizi, A., Wang, H., Cox, D., Cramer, L. A., & Dong, S. (2017). Agent-based tsunami evacuation modeling of unplanned network disruptions for evidence-driven resource allocation and retrofitting strategies. *Natural Hazards*, 88(3), 1347–1372.
- Mostafizi, A., Wang, H., Cox, D., & Dong, S. (2019). An agent-based vertical evacuation model for a near-field tsunami: Choice behavior, logical shelter locations, and life safety. *International Journal of Disaster Risk Reduction*, 34, 467–479.
- Motter, A. E., & Lai, Y.-C. (2002). Cascade-based attacks on complex networks. Physical Review E, 66(6), 065102.
- Murphy, C., & Gardoni, P. (2008). The acceptability and the tolerability of societal risks: A capabilities-based approach. *Science and Engineering Ethics*, 14(1), 77–92.
- Murray, A. T., & Grubesic, T. H. (2007). Overview of reliability and vulnerability in critical infrastructure. *Critical infrastructure* (pp. 1–8). Springer.
- Nagurney, A., & Qiang, Q. (2009). A relative total cost index for the evaluation of transportation network robustness in the presence of degradable links and alternative travel behavior. *International Transactions in Operational Research*, 16(1), 49–67.
- Novak, D. C., & Sullivan, J. L. (2014). A link-focused methodology for evaluating accessibility to emergency services. Decision Support Systems, 57, 309–319.
- Ogie, R. I., Holderness, T., Dunn, S., & Turpin, E. (2018). Assessing the vulnerability of hydrological infrastructure to flood damage in coastal cities of developing nations. Computers, Environment and Urban Systems, 68, 97–109.
- Östh, J., Reggiani, A., & Galiazzo, G. (2015). Spatial economic resilience and accessibility: A joint perspective. *Computers, Environment and Urban Systems, 49*, 148–159.
- Parenteau, M.-P., & Sawada, M. C. (2011). The modifiable areal unit problem (maup) in the relationship between exposure to no_2 and respiratory health. *International Journal of Health Geographics*, 10(1), 58.
- Paton, D., McClure, J., & Bürgelt, P. T. (2006). Natural hazard resilience: The role of individual and household preparedness. Disaster Resilience: An Integrated Approach, 105, 27.
- Peacock, W. G. (2003). Hurricane mitigation status and factors influencing mitigation status among floridas single-family homeowners. *Natural Hazards Review*, 4(3), 149–158.
- Peacock, W. G., Dash, N., & Zhang, Y. (2007). Sheltering and housing recovery following disaster. *Handbook of disaster research* (pp. 258–274). Springer.
- Perry, R. W., Lindell, M. K., & Tierney, K. J. (2001). Facing the unexpected: Disaster preparedness and response in the United States. Joseph Henry Press.
- Petersen, L., Fallou, L., Reilly, P., & Serafinelli, E. (2018). Public expectations of critical infrastructure operators in times of crisis. Sustainable and Resilient Infrastructure, 1–16.

- Poorzahedy, H., & Bushehri, S. N. S. (2005). Network performance improvement under stochastic events with long-term effects. *Transportation*, 32(1), 65–85.
- Pregnolato, M., Ford, A., Wilkinson, S. M., & Dawson, R. J. (2017). The impact of flooding on road transport: A depth-disruption function. *Transportation Research Part D: Transport and Environment*, 55, 67–81.
- Price, R., & Vojinovic, Z. (2008). Urban flood disaster management. *Urban Water Journal*, 5(3), 259–276.
- Radicchi, F. (2015). Percolation in real interdependent networks. *Nature Physics*, 11(7), 597.
- Robinson, A. C., & Quinn, S. D. (2018). A brute force method for spatially-enhanced multivariate facet analysis. Computers, Environment and Urban Systems, 69, 28–38.
- Sakakibara, H., Kajitani, Y., & Okada, N. (2004). Road network robustness for avoiding functional isolation in disasters. *Journal of Transportation Engineering*, 130(5), 560, 567.
- Schneider, C. M., Moreira, A. A., Andrade, J. S., Havlin, S., & Herrmann, H. J. (2011).
 Mitigation of malicious attacks on networks. Proceedings of the National Academy of Sciences. 108(10), 3838–3841.
- Shao, S., Huang, X., Stanley, H. E., & Havlin, S. (2015). Percolation of localized attack on complex networks. New Journal of Physics, 17(2), 023049.
- Shinn, M., Knickman, J. R., & Weitzman, B. C. (1991). Social relationships and vulnerability to becoming homeless among poor families. *American Psychologist*, 46(11), 1180.
- Solé, R. V., Rosas-Casals, M., Corominas-Murtra, B., & Valverde, S. (2008). Robustness of the european power grids under intentional attack. *Physical Review E*, 77(2), 026102.
- Sullivan, J., Aultman-Hall, L., & Novak, D. (2009). A review of current practice in network disruption analysis and an assessment of the ability to account for isolating links in transportation networks. *Transportation Letters*, 1(4), 271–280.
- Tahmasbi, B., & Haghshenas, H. (2019). Public transport accessibility measure based on weighted door to door travel time. Computers, Environment and Urban Systems, 76, 163–177
- Tamima, U., & Chouinard, L. (2017). Systemic seismic vulnerability of transportation networks and emergency facilities. *Journal of Infrastructure Systems*, 23(4), 04017032.
- Tierney, K. J., Lindell, M. K., & Perry, R. W. (2002). Facing the unexpected: Disaster preparedness and response in the United States. *Disaster Prevention and Management:* An International Journal, 11(3), 222.
- Vandenbulcke, G., Steenberghen, T., & Thomas, I. (2009). Mapping accessibility in Belgium: A tool for land-use and transport planning. *Journal of Transport Geography*, 17(1), 39–53.
- Vespignani, A. (2010). Complex networks: The fragility of interdependency. *Nature*, 464(7291), 984–985.
- Wang, M., & Mu, L. (2018). Spatial disparities of uber accessibility: An exploratory analysis in Atlanta. Usa. Computers. Environment and Urban Systems. 67, 169–175.
- Wang, W., Yang, S., Stanley, H. E., & Gao, J. (2019). Local floods induce large-scale abrupt failures of road networks. *Nature Communications*, 10(1), 2114.
- Wang, Z., Chan, A. P., Yuan, J., Xia, B., Skitmore, M., & Li, Q. (2014). Recent advances in modeling the vulnerability of transportation networks. *Journal of Infrastructure Systems*, 21(2), 06014002.
- Yin, J., Yu, D., Yin, Z., Liu, M., & He, Q. (2016). Evaluating the impact and risk of pluvial flash flood on intra-urban road network: A case study in the city center of shanghai, China. *Journal of Hydrology*, 537, 138–145.
- Zahran, S., Brody, S. D., Peacock, W. G., Vedlitz, A., & Grover, H. (2008). Social vulnerability and the natural and built environment: A model of flood casualties in Texas. *Disasters*, 32(4), 537–560.
- Zhao, J., Li, D., Sanhedrai, H., Cohen, R., & Havlin, S. (2016). Spatio-temporal propagation of cascading overload failures in spatially embedded networks. *Nature Communications*, 7, 10094.